From the Department of Pathobiology

University of Veterinary Medicine Vienna

Institute of Virology

(Head: Univ.-Prof. Dr.med.vet. Till Rümenapf)

An influence of m6A methylation on the infectivity of mouse mammary tumor virus

Master thesis

University of Veterinary Medicine Vienna

Submitted by

Tanja Kusstatscher, BSc

01316372

Vienna, July 2023

Supervisor: Stanislav Indik, PhD

Reviewer: Ao.Univ.-Prof. Dr.med.vet. Dieter Klein

Statutory Declaration

"I declare in lieu of an oath that I have written this master thesis myself and that I have not used any sources or resources other than stated for its preparation. I further declare that I have clearly indicated all direct and indirect quotations. This master thesis has not been submitted elsewhere for examination purposes."

Date: 14.07.2023

Tanja KUSSTATSCHER

Acknowledgments

First and foremost, I want to thank Stanislav Indik, PhD for giving me the chance to in his laboratory at the Institute of Virology, University of Veterinary Medicine, Vienna. Through his supervision I was able to learn many different laboratory techniques and gain a lot of knowledge in the field of virology. Thank you!

As well as I would like to thank the whole staff of the Institute of Virology for their support.

Finally, I want to thank my friends for their emotional support and my family for their financial support.

Abstract

Numerous epitranscriptomic modifications were identified in cellular and viral mRNAs. The most common modification is the methylation of the Adenosine (m6A) that is deposited onto mRNA with the help of a cellular enzyme, methyl transferase METTL3. The presence of the N6-methyladenosine in mRNA was proposed to influence various aspects of the mRNA life cycle including the stability, splicing, nuclear export, and translation.

Viruses hijack cellular pathways to facilitate the nucleo-cytoplasmic transport of viral RNAs. They serve as excellent model organisms to study RNA transport as they contain cis-acting sequence elements recognized by cellular nuclear export factors. Recent reports showed that the m6A modifications in the retroviral mRNAs have some effect on the viral gene expression levels and ultimately on virus infectivity. However, the mechanism responsible for this observation and the importance for the virus life cycle remains controversial.

We hypothesized that the m6A methylation influences the interaction between retroviral RNA and cellular nuclear RNA export factors thereby affecting the translocation of viral RNA into the cytoplasm and resulting in reduced production of viral particles and loss of infectivity. To test this hypothesis, we knocked out the Mettl3 gene from the human genome by using the CRISPR/Cas9 system and used modified and control cells to produce a prototypic mouse retrovirus mouse mammary tumor virus (MMTV) to monitor changes in the virus infectivity. Furthermore, we used the METTL3-lacking cells to determine the nuclear RNA export efficiency using a GFP-based nuclear export assay previously established in the laboratory. In this assay, we tested the methylation-dependent activity of three export elements: 1) the Rev-response element from HIV-1 (RRE, in conjunction with the trans-acting factor Rev), 2) the constitutive transport element (CTE) from Mason-Pfizer monkey virus (MPMV) and 3) a novel cis-acting RNA element, derived from the 5’ end of MMTV env mRNA, MPPE.

We did not observe a reduced infectivity of MMTV produced in cells lacking METTL3 compared to the virus produced in wild-type cells. Furthermore, no significant difference in mRNA export between the wild-type and knockout groups could be detected with neither of the export elements. A tendency of reduced mRNA export in the knockout group is visible for some export elements.

In conclusion, we did not observe any influence on retroviral mRNA nuclear export and MMTV infectivity caused by the m6A modification.

Zusammenfassung

Zahlreiche epitranskriptomische Modifikationen wurden in zellulären und viralen mRNAs identifiziert. Die häufigste Modifikation ist die Methylierung des Adenosins (m6A), die mit Hilfe eines zellulären Enzyms, der Methyltransferase METTL3, an die mRNA angehängt wird. Es wurde vermutet, dass das Vorhandensein von N6-Methyladenosin an mRNA verschiedene Aspekte des mRNA-Lebenszyklus beeinflusst, unteranderem Stabilität, Spleißen, Export aus dem Zellkern und Translation.

Viren nutzen zelluläre Signalwege, um den nukleozytoplasmatischen Transport viraler RNAs zu erleichtern. Sie dienen als hervorragende Modellorganismen zur Untersuchung des RNA-Transports, da sie cis-aktive Sequenzelemente enthalten, die von zellulären nukleären Exportfaktoren erkannt werden. Jüngste Berichte zeigten, dass die m6A-Modifikationen in den retroviralen mRNAs einen gewissen Einfluss auf die viralen Genexpressionsniveaus und letztendlich auf die Virusinfektiosität haben. Der für diese Beobachtung verantwortliche Mechanismus und die Bedeutung für den Viruslebenszyklus bleiben jedoch umstritten.

Wir haben die Hypothese aufgestellt, dass die m6A-Methylierung die Wechselwirkung zwischen retroviraler RNA und zellulären nukleären RNA-Exportfaktoren beeinflusst und dadurch die Translokation viraler RNA in das Zytoplasma beeinflusst, was zu einer verringerten Produktion viraler Partikel und einem Verlust der Infektiosität führt. Um diese Hypothese zu testen haben wir das *Mettl3*-Gen aus dem menschlichen Genom mittels des CRISPR/Cas9-Systems ausgeschaltet und modifizierte sowie Kontrollzellen verwendet, um ein prototypisches Retrovirus, das Maus-Mammary-Tumorvirus (MMTV), zu produzieren und Veränderungen in der Infektiosität des Virus festzustellen. Darüber hinaus haben wir Zellen ohne funktionsfähiges METTL3-Gen verwendet, um die Effektivität der nuklearen RNA-Exportes zu bestimmen. Dies wurde mithilfe eines im zuvor etablierten GFP-basierten nuklearen Exportassays, gemacht. In diesem Assay haben wir die methylierungsabhängige Aktivität von drei Exportelementen getestet: 1) das Rev-Response-Element von HIV-1 (RRE, in Verbindung mit dem trans-wirkenden Faktor Rev), 2) das konstitutive Transportelement (CTE) vom Mason-Pfizer-Affenvirus (MPMV) und 3) ein neues cis-wirkendes RNA-Element, abgeleitet vom 5'-Ende der MMTV-env-mRNA, MPPE.

Wir haben keine verringerte Infektiosität von MMTV beobachtet, dass in Zellen ohne METTL3 produziert wurde, verglichen mit dem Virus, das in Wildtyp-Zellen produziert wurde. Darüber

hinaus konnte mit keinem der Exportelemente ein signifikanter Unterschied im mRNA-Export zwischen der Wildtyp- und der Knockout-Gruppe festgestellt werden. Bei einigen Exportelementen ist eine Tendenz zu einem verringerten mRNA-Export in der Knockout-Gruppe erkennbar.

Zusammenfassend haben wir keinen Einfluss der m6A-Modifikation auf den nukleären Export retroviraler mRNA und die Infektiosität von MMTV festgestellt.

Table of content

List of Figures and Tables

Abbreviations

AlkBH5	alkB homolog 5
CA	Capsid
CAE	cytoplasmic accumulation element
Cas9	CRISPR associated protein 9
CBC	Cap binding complex
CRIM1	chromosome region maintenance protein 1
CRISPR	Clustered regularly interspaced short palidromic repeats
CTE	constitutive transport elements
EJC	exon junction complex
FG	containing phenylalanine-glycine repeats or FG-repeats
FTO	FTO alpha-ketoglutarate dependent dioxygenase
hnRNAPA2B1	Heterogeneous nuclear ribonucleoprotein A2/B1
hnRNPC	Heterogeneous nuclear ribonucleoprotein C
hnRNPG	Heterogeneous nuclear ribonucleoprotein G
IAP	intracisternal A-type particle
IAPEs	IAP expression elements
ICE	Inference of CRISPR edits
IGF2BP	insulin-like growth factor 2
IN	Integrase
KO	Knock-out
lncRNA	Long-chain non-coding RNA
LRR	leucine-rich repeat

LTR	Long terminal repeats
m6A	Methylation of adenosine at the N6 position
MA	Matrix
METTL14	Methyl transferase 14
METTL3	Methyl transferase 3
MMTV	Mouse Mammary Tumor Virus
MPMV	Mazon-Pfizer Monkey Virus
MPPE	MMTV positive posttranscriptional element
mRNA	Messenger RNA
mRNP	messenger ribonucleoprotein
NC	Nucleocapsid
NES	Nuclear export signals
NHEJ	Non-homologous end joining
NLS	Nuclear localization signals
NLTF2	nuclear transport factor 2-like domain
NPC	Nuclear pore complex
nups	Nucleoporins
NXF1	Nuclear RNA export factor 1
NXT1	NTF2-related export protein 1
PAM	Protospacer-adjacent motiv
PIC	Pre-integration complex
PR	Proteas
P-TEFb	positive transcription elongation factor b
RBM15	RNA-binding motif protein 15

RNAP II	RNA polymerase II
RRE	Rev-response element
RRM	N-terminal RNA recognition motif
rRNA	Ribosomal RNA
RT	Transcriptase
RTE	RNA transport element
sncRNA	Non-coding small RNA
SRV	simian retroviruses
SU	Surface protein
Tat	HIV-1 transactivator of transcription
TM	Transmembrane protein
TREX	transcription-export complex
tRNA	Transfer RNA
UBA	ubiquitin-associated
VIRMA	vir-like m6A methyltransferase associated
WTAP	Wilms tumor 1-associated protein
YTHDC1	YTH domain containing 1
YTHDC2	YTH domain containing 2
YTHDF1	YTH domain-containing family protein 1
YTHDF2	YTH domain-containing family protein 2
ZCH13	Zinc finger CCHC domain-containing protein 13

1 INTRODUCTION

1.1 Methylation

Posttranscriptional modifications represent an important mechanism for providing additional information beyond the information carried by the RNA sequence. At present, over 100 various posttranscriptional modifications on RNA transcripts have been identified in messenger RNA (mRNA), transfer RNA (tRNA), ribosomal RNA (rRNA), non-coding small RNA (sncRNA) and long-chain non-coding RNA (lncRNA). Most of these modifications were found in tRNA (1). Approximately 10 epitranscriptiomic modification were identified in mRNA, with the methylation of adenosine at the N6 position (m6A) being the most frequent and also most studied modification of mRNA (2). This modification is highly conserved from plants to mammals (3). It is widely accepted that the RNA methylation represents an important layer of the post-transcriptional regulation of gene expression. It plays an important role in development as a loss of m6A can block the differentiation of mammalian embryonic stem cells (4, 5).

The m6A methylations of mRNA are performed in the nucleus. The methylation is catalysed by a “writer” complex, which consists of several proteins including methyl transferase 3 (METTL3), methyl transferase 14 (METTL14), Wilms tumor 1-associated protein (WTAP), vir-like m6A methyltransferase associated (VIRMA), Zinc finger CCHC domain-containing protein 13 (ZCH13) and RNA-binding motif protein 15 (RBM15). The METTL3 has the catalytic role, which is supported by the other cofactors. For example, MELLT14 functions as a structural support and assists in RNA substrate binding. WTAP is required for stabilization of the core complex and the RBM15 guides the methylation complex to its targeted RNA (6, 7). The m6A methylation occurs in a specific sequence context. Specifically, m6A methylation were mapped to the RRACH (R = A or G, H = A,C, or U) sequence motif (8).

Beside the “writers”, other proteins are able to detect (read) the m6A residues in mRNA. The number protein “readers” able to recognize the m6A mark is permanently growing. Historically, the first identified “m6A readers” consisted of proteins containing YTH domains such as YTH domain containing 1 (YTHDC1), YTH domain containing 2 (YTHDC2), YTH domain-containing family protein 1 (YTHDF1), YTH domain-containing family protein 2 (YTHDF2). In recent years, researchers have discovered that also the abundantly expressed heteronuclear

ribonucleoproteins including heterogeneous nuclear ribonucleoprotein C (hnRNPC), heterogeneous nuclear ribonucleoprotein G (hnRNPG), and heterogeneous nuclear ribonucleoprotein A2/B1 (hnRNPA2B1), and insulin-like growth factor 2 (IGF2BP) recognize the m6A-modified RNA (9). Binding of the “readers” onto mRNA effects various stages of the mRNA life cycle. For example, binding of YTHDF1 to mRNA promotes its translation. On the other hand, binding of YTHDF2 will lead to the degradation of mRNA. It is also believed that the interaction of m6A-mRNA with hnRNPC results in changes in the alternative splicing. (10). A recent body of evidence also suggests that m6A modification of mRNA facilitates its recognition by nuclear export adaptors thereby providing a link to the nuclear export machinery. The most comprehensive evidence was provided for the YTHDC1 nuclear reader protein that interacts with a nuclear export adaptor protein SRSF3 and thereby facilitates interaction with the major nuclear export receptor, Nuclear RNA export factor 1 (NXF1) (11). Further evidence for an involvement of m6A modification in mRNA nuclear export was reported for the core member of the “writer” complex, RBM15. The protein in known as a bona fide member of the NXF1 mRNA export complex (12). Thus, is seems conceivable that binding of RBM15 onto mRNA during m6A methylation function as a mediator between the methylation and mRNA export machinery.

Apart from the m6A and “readers”, m6A-modified mRNA can be recognized by m6A “erasers” (demethylases). The demethylation of m6A is performed by the RNA demethylases alkB homolog 5 (AlkBH5) and FTO alpha-ketoglutarate dependent dioxygenase (FTO) (13). Figure 1.

Through new technologies a high level of m6A could be shown on mRNA of DNA and RNA viruses too. It is anticipated that m6A affect the mRNA splicing, translation and export. It also influences several parts of the viral life cycle and has therefore a significant impact on the phenotype (14).

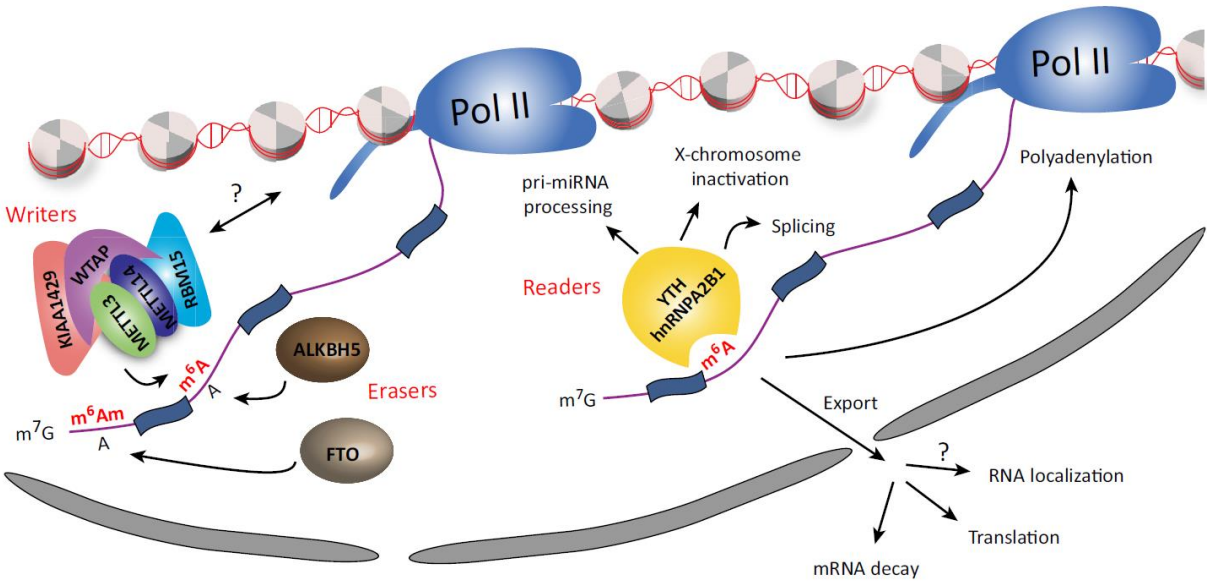

Figure 1: Writer, reader, and eraser of m6A. Figure modified from (3)*:* The m6A writer is composed of a minimum of five proteins, one of which is the catalytic subunit methyltransferase 3 (METTL3). METTL14 acts as a structural support for METTL3, while Wilmstumor1-associated protein (WTAP) stabilizes the core complex. RNA-binding motif protein 15 (RBM15) assists in recruiting the complex to its target sites. Two demethylases, ALKB homolog 5 (ALKBH5) and FTO alpha-ketoglutarate dependent dioxygenase (FTO), are responsible for removing the methyl group from m6A and 20-O-ribose methylated m6A (m6Am), respectively. m6A readers consist of heterogeneous nuclear ribonucleoprotein (hnRNP) A2B1 and various members of the YTH-domain protein family. These factors facilitate the functioning of m6A in various processes, including X-chromosome inactivation.

1.2 Nuclear export of cellular mRNA

After transcription, mRNA matures and must be transported from the nucleus into the cytoplasm. Nucleus and cytoplasm are connected through the nuclear pore complex (NPC). The NPC plays a central role in the selective transport between these two compartments. The NPCs are octagonal structures that consist of a central cylindrical channel, cytoplasmic filaments, and a nuclear basket. It is composed of approximately 30 different proteins known as nucleoporins (nups), which can be categorized into three groups. The membrane nups anchor the NPCs to the nuclear envelope, the scaffolding nups shape the central structure of

the NPCs, and the FG nups (containing phenylalanine-glycine repeats or FG-repeats) play a role in the transportation of cargo through the central channel (15–17).

While the NPCs allow the small molecules (<26kDa) to pass through the pore via diffusion, the active transport, which requires energy and is directional, is required for larger molecules. The active transport primarily involves a group of conserved nuclear transport receptors known as karyopherins. Karyopherins play a crucial role in shuttling proteins to and from the nucleus by recognizing specific short peptide signals called nuclear localization signals (NLS) or nuclear export signals (NES). Additionally, karyopherins can also recognize nucleotide motifs, enabling them to export specific RNA molecules from the nucleus. To transport protein and RNA cargos through NPCs, karyopherins interact directly with FG nucleoporins and utilize a RanGTP-RanGDP gradient across the nuclear membrane as the driving force. The importins are karyopherins responsible for importing cargo into the nucleus, while the exportins are karyopherins involved in exporting cargo out of the nucleus (18). The typical nuclear export of macromolecule cargoes involves three steps: docking onto the nuclear basket, transit through the central channel of the NPC, and release at the cytoplasmic filaments. Once the mRNA cargoes have reached the cytoplasm, export receptors containing NLS are translocated back to the nucleus to repeat the process (16, 19).

The most important member of the karyopherin family is “chromosome region maintenance protein 1” (CRM1), also known as Exportin 1. CRM1 is the major export receptor for several macromolecules such as proteins and diverse kinds of RNA, including some mRNAs and snRNAs (20).

Karyopherin independent export is mediated by the transcription-export complex (TREX). TREX is a highly conserved multiprotein complex that plays a crucial role in connecting the transcription of messenger RNAs with their nuclear export. This mediation starts already with the processing of pre-mRNA (21). During early steps of the formation of messenger ribonucleoprotein complexes (mRNPs) a subset of TREX1 complex proteins, including THO and the adapter ALY and UAP56, bind to the mRNA. Specifically, the proteins bind to the first exon junction complex (EJC) that is formed during splicing. These subunits also bind to the cap-binding complex (CBC) that recognizes the caped mRNA (22). As soon as the TREX1 is assembled at the mRNA the NXF1 and its co-factor NTF2-related export protein 1 (NXT1) are recruited to the mRNP. Subsequently, the NXF1/NXT1 heterodimer, previously known as Tap/p15, interacts with TREX2 and mediates the interaction of the complex with the NPC. Here,

the mRNP is exported through the interaction of NXF1–NXT1 with FG-nups inside the NPC pore (23, 24).

NXF1 consist of 4 domains including an N-terminal RNA recognition motif (RRM), a leucine-rich repeat (LRR), a nuclear transport factor 2-like domain (NTF2L) and an ubiquitin-associated (UBA) domain (25). The NXT1 is a smaller protein that also has an NTF2-like fold and forms a heterodimer with NXF1 via the NTF2L domain. The NTF2L and UBA domain both interact with the FG motifs in the nups and facilitate mRNA export (26, 25, 27).

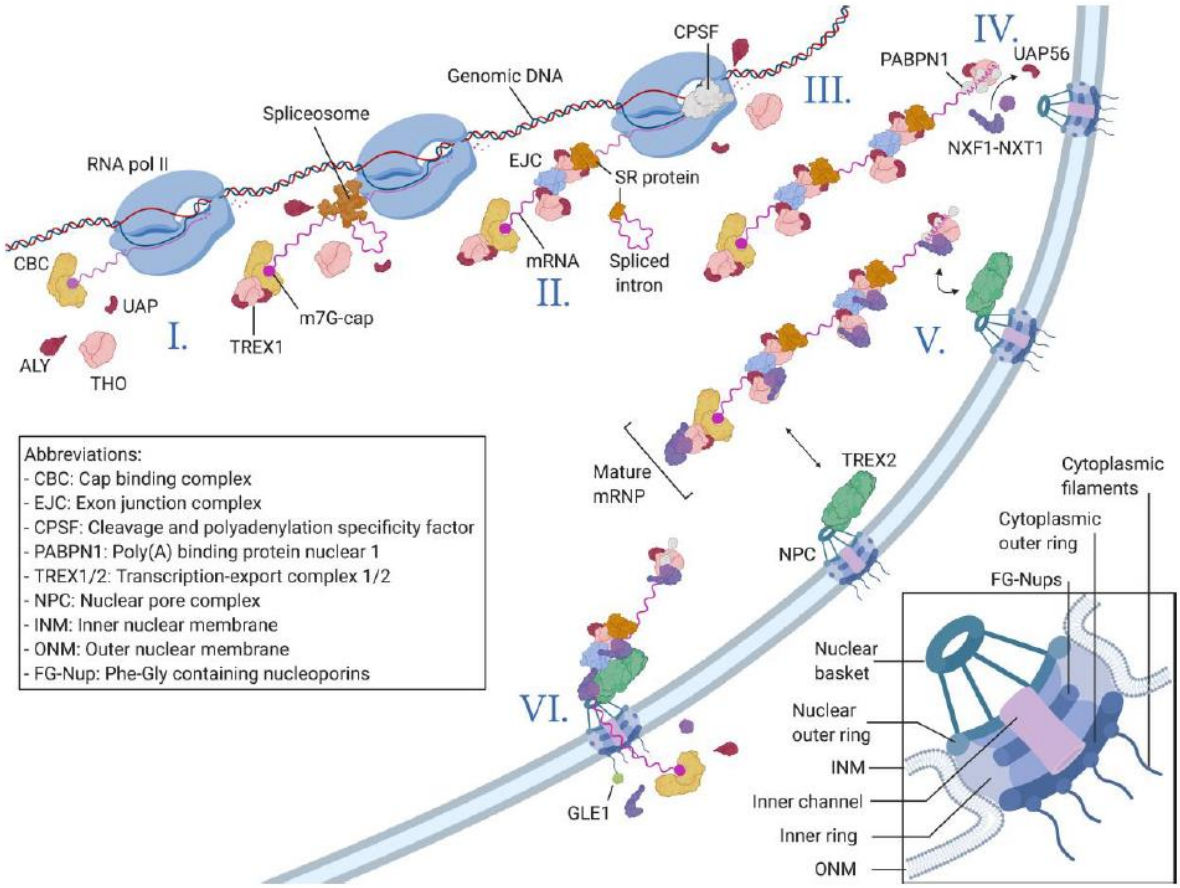

Figure 2: Karyopherin independent pathway with TREX. Modified from (19): **I**. Transcription Initiation: RNA polymerase II begins transcribing the genomic DNA and generates a capped transcript. The cap is recognized by the cap-binding complex (CBC). The TREX core complex, which includes THO and the adapters ALY (Ally of AML-1 and LEF-1) and UAP56, assembles at the CBC. **II**. Splicing: The spliceosome assembles at the splicing sites of the nascent mRNA and facilitates the removal of introns. The exon junction complex (EJC) is deposited 23 nucleotides upstream of the splicing site, where Serine-Arginine-rich (SR) proteins remain attached to the mRNA. The TREX1 complex interacts with

the EJC and SR proteins. **III**. Cleavage and Polyadenylation: The cleavage and polyadenylation specificity factor complex (CPSF) cleaves the nascent mRNA at termination sites and promotes the synthesis of the poly(A) tail. **IV**. Recruitment of Export Factors: Nuclear RNA export factor 1 (NXF1)–NTF2-related export protein 1 (NXT1) exportins are recruited by the TREX1 complex, starting at the 3' end of the mature mRNA. **V**. Export through Nuclear Pore Complex: NXF1–NXT1 interact with TREX2 to guide the mature mRNA-protein complex (mRNP) towards the nuclear pore complex (NPC). The mRNP is then exported through the interaction of NXF1–NXT1 with FG-Nups inside the NPC pore. **VI**. Protein Dissociation and Recycling: During export, numerous protein components of the mRNP are removed, while others dissociate from the mRNA in the cytoplasm and are recycled back to the nucleus. A detailed representation of the nuclear pore complex is provided in the square at the bottom right corner.

1.3 Processing and nuclear export of retroviral mRNAs

Retroviruses are cellular parasites that contain the single-stranded, plus-sense RNA as their genome. The viral RNA is surrounded by a nucleocapsid protein, a protein capsid core and an envelope. Following reverse transcription of the viral RNA, the newly synthesized viral DNA is integrated into the host genome. Due to the small size of the retroviral genome, the expression of viral proteins is highly dependent on cellular machinery. The ability to hijack cellular pathways including those that regulate the RNA expression at the post-transcriptional levels allowed to use retroviruses as an excellent model system to study nuclear export (28). In fact, retroviruses have been used to gain key insights into the mechanisms involved in the export of RNA from the nucleus.

To initiate infection, retroviruses use the envelope glycoprotein, present on the surface of virions, to interact with a specific host cell surface receptor(s) and mediate fusion of the viral envelope with the cell membrane. After fusion, the viral capsid is released into the cytoplasm where the genomic RNA is reverse transcribed into double-stranded DNA by the virus-encoded reverse transcriptase. During this process, the reverse transcriptase undertakes two essential transitions, moving from the 5' terminus to the 3' terminus. These results in a duplication of the sequences located at both ends of the template RNA molecule, and formation of long terminal repeats (LTR). These repeats contain promoter and enhancer sequences that initiate viral transcription, as well as termination sequences necessary for 3' end processing. The double-stranded DNA interacts with capsid proteins and the viral integrase to form the pre-integration

complex (PIC). The PIC then moves to the nucleus, where the viral integrase facilitates the integration of viral genetic information into the host genome, forming a provirus (28).

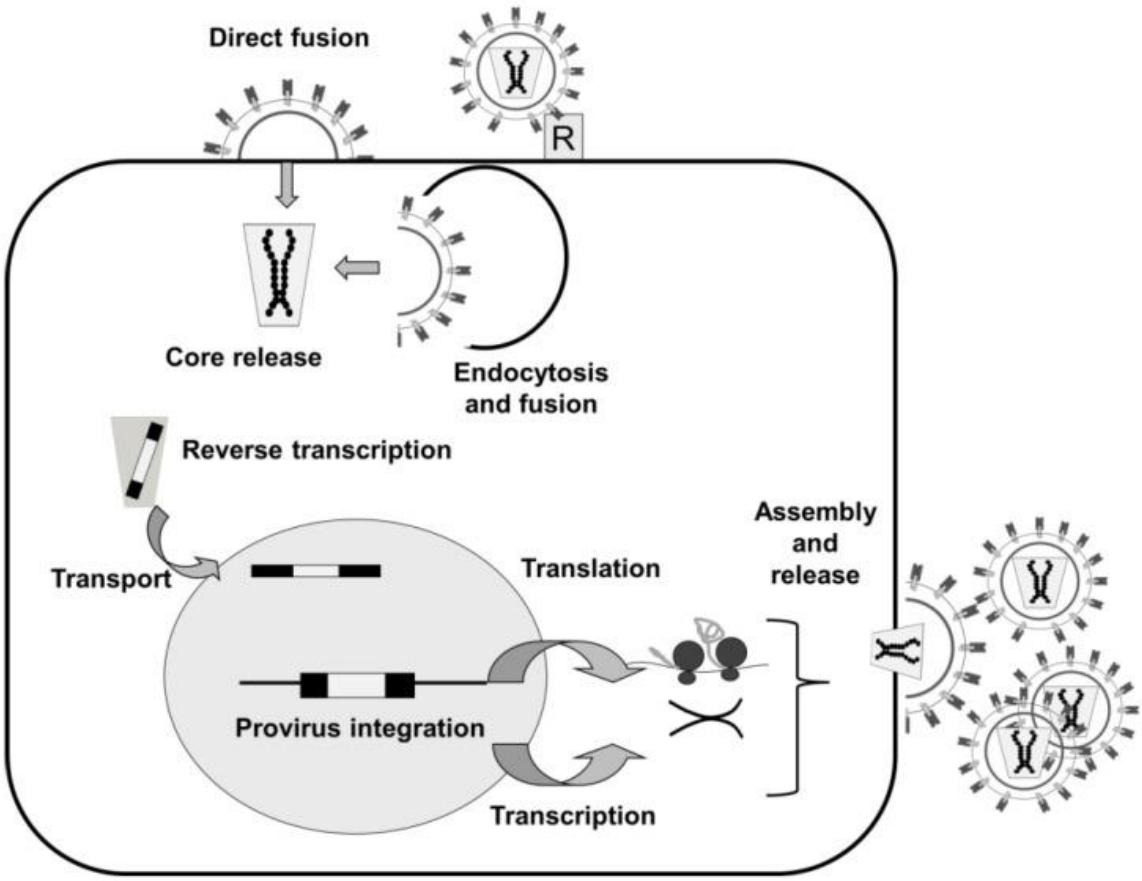

Figure 3: Simplified retroviral lifecycle. Modified from (29)*:* At the top, the retrovirus particle interacts with a receptor on the cell membrane (represented as "R"). Following receptor engagement, the virus can enter the cell in two ways: either through direct fusion with the cell membrane ("Direct fusion") or through receptor-mediated endocytosis and subsequent membrane fusion ("Endocytosis and fusion"). The internal core of the virus is then released ("Core release"), and the RNA contained within the core undergoes reverse transcription, resulting in the generation of a single cDNA copy ("Reverse transcription"). In the case of lentiviruses, the entire core, including the cDNA, is actively transported to the nucleus ("Transport") and integrated into the cell chromosomes as a provirus ("Provirus integration"). Once inside the host cell, the retrovirus exploits the cellular transcriptional machinery to ensure the production of its own mRNA, which is then translated in the cytoplasm. The newly synthesized viral proteins encapsidate a full-length copy of the viral genome and assemble into new virus particles. These newly formed viral particles are then released from the cell and can spread to neighbouring cells, continuing the infection cycle.

All retroviruses contain three genes including *gag, pol* and *env*. The *gag* gene is at the 5' end and encodes for the structural proteins forming the core, matrix (MA), capsid (CA) and nucleocapsid (NC). The *gag* gene is followed by the *pol* gene. The *pol* gene encodes the viral enzymes, including reverse transcriptase (RT), integrase (IN) and protease (PR). The *env* gene encodes the surface (SU) and transmembrane (TM) proteins responsible for receptor binding and membrane fusion, respectively (28).

Retroviruses can be broadly divided into simple and complex viruses. The simple retroviruses contain only the three main coding regions. On the other hand, complex retroviruses express one or more accessory proteins. These additional proteins are expressed from multiply spliced viral RNA species.

The provirus is transcribed by the cellular RNA polymerase II (RNAP II), which binds to the viral promoter (enhancer) located in the 5' LTR. Simple retroviruses control their transcription by interaction of cellular factors with the LTR site. In contrast, complex retroviruses control transcription with self-encoded *trans*-acting factors, such as the HIV-1 transactivator of transcription (Tat) (30). Tat, together with the cellular positive transcription elongation factor b (P-TEFb) complex, binds to the viral TAR sequence at the 5 'end of nascent viral RNA. Binding leads to the phosphorylation of the RNAP II, allowing synthesis of the full-length viral RNAs (31).

After transcription, viral mRNA is capped at the 5' end poly-Adenylated at the 3' end. A proportion of the viral RNA synthesized is spliced to produce mRNA encoding the SU and TM and the accessory proteins. The spliced RNA can be exported from the nucleus via the TREX-NXF1/NXT1 pathway. However, retroviruses are faced with the problem that they also have to export the unspliced RNA that encodes the viral structural components and serves as the viral genome. The nuclear export of the intron-containing mRNAs is normally prevented by cellular machinery. Thus, retroviruses have to overcome the cellular nuclear retention mechanism which prevents incompletely spliced RNA from exiting the nucleus. To overcome this process retroviral RNA contains cis-acting sequences that hijack the cellular nuclear export machinery. The sequences and the cellular binding partners differ between simple and complex retroviruses (28, 32).

1.3.1 Nuclear export of simple retroviruses

Simple retroviruses lack additional accessory proteins that regulate their gene expression. Instead, they rely solely on cis-acting RNA elements to recruit cellular export receptors and adaptors to the intron-containing genomic RNA transcripts.

Type D retroviruses, such as Mazon-Pfizer Monkey Virus (MPMV) and simian retroviruses (SRV) type 1 and 2, played a pivotal role in the identification of the RNA nuclear export mechanisms. In the mid-1990s, it was recognised that these viruses have a cis-acting sequence that drives the transport of viral RNA across the nuclear pore complex (33). The sequence was named the constitutive transport elements (CTEs). These CTEs are found in the noncoding regions of their unspliced transcripts and directly facilitate RNA nuclear export by interacting with the NXF1 protein (33, 34). The Identification of NXF1 as the binding partner of the CTEs was one of the most important discoveries in the molecular biology field as it turned out that NXF1 is the major nuclear exporter responsible for the transport of cellular bulk mRNAs to the cytoplasm. The LRR domains of NXF1 associate with the RRM domains to bind a conserved secondary structure in the CTE. Specifically, NXF1 associates with an extended hairpin loop with four conserved internal loops. These loops, arranged in two mirror-symmetric pairs, serve as core binding sites for NXF1. The double stranded regions of the CTE are formed by non-conserved sequences and do not directly participate in NXF1 binding (35, 36). Additionally, the RNA helicase A has been demonstrated to interact with CTE to enhance the interaction with NXF1 (37). Cis-acting nuclear export sequences similar to the D-type retrovirus CTEs, have been identified in rodent intracisternal A-type particle (IAP) retroelements. The sequences were named CTE_{iap} and IAP expression elements (IAPEs). Type D and type A CTEs share a conserved secondary structure with core binding motifs for NXF1 (38).

The IAPs also contain another family of *cis*-acting RNA export elements called RNA transport elements (RTEs), which are structurally distinct from CTEs. Like CTEs, RTE-mediated nuclear export is not dependent on the cellular karyopherin CRM1, as RTE-containing RNA has been observed to exit the nucleus in the presence of leptomycin B, an inhibitor of the CRM1 pathway. Furthermore, the RTE segment does not show a high affinity for NXF1 (39). A recent study revealed that RTE-containing transcripts are exported via a NXF1-mediated pathway utilizing RBM15 as an adaptor protein to facilitate RNA association with NXF1 (12).

Recently, it has been reported that gammaretroviruses, such as murine leukemia virus (MLV) and xenotropic murine leukemia virus (XMRV), also possess a conserved cis-acting nuclear export element called cytoplasmic accumulation element (CAE). Like CTE, CAE directly interacts with NXF1 to facilitate nuclear export of unspliced viral transcripts (40).

1.3.2 Nuclear export mechanism of complex retroviruses

The accessory proteins of complex retroviruses have diverse functions, including facilitating the nuclear export of viral RNAs. The transcripts encoding these auxiliary proteins undergo multiple splicing events to enable their transportation to the cytoplasm where they are translated by the host cell machinery. These RNA transport proteins possess both nuclear localization and nuclear export signals, allowing them to move between the nucleus and the cytoplasm. Within the nucleus, they specifically bind to a *cis*-acting RNA element present in singly spliced and unspliced viral transcripts, facilitating their export from the nucleus.

The first identified virus-encoded trans-acting RNA export factor was the HIV-1 Rev protein (41, 32). Rev targets a highly structured region called the Rev-response element (RRE), located within the *env* gene of the HIV-1 genome. Multiple Rev molecules bind to a single RRE, which is found in both singly spliced and unspliced HIV-1 transcripts. Rev, in association with viral RNAs, mediates the nuclear export of the complex through a CRM1-dependent pathway (42, 43). The Rev/CRM1 activity requires the ATP-dependent DEAD box RNA helicase known as DDX3 (44). Apart from its role in nuclear export, Rev also interacts with the cellular splicing factor SF2/ASF, thereby regulating splicing (45). Furthermore, Rev has been found to promote the encapsidation of HIV-1 RNAs into viral particles and enhance the efficiency of translation of specific RNAs (46). Consequently, Rev demonstrates to be a multifunctional *trans*-acting factor.

In addition to HIV-1, other primate immunodeficiency viruses such as HIV-2 and simian immunodeficiency virus (SIV) encode Rev proteins that bind to RRE sequences to regulate gene expression (47). Rev-like proteins have also been discovered in the genomes of non-primate lentiviruses like equine infectious anemia virus (EIAV), feline immunodeficiency virus (FIV), and bovine immunodeficiency virus (BIV) (48–50). Moreover, similar gene expression regulators resembling HIV-1 Rev have been identified in retroviruses of the deltaretrovirus and betaretrovirus genera. Human T-cell leukemia virus 1 (HTLV-1), a prototypic deltaretrovirus,

encodes the trans-acting factor Rex, which specifically targets the highly structured Rex-response element (RxRE) (51). Additionally, a Rev-like protein known as Rem, which interacts with a Rem-response element (RmRE), has been found in the genome of the prototypic betaretrovirus MMTV. The identification of the Rev orthologue in the MMTV genome resulted in the reclassification of MMTV from a simple to a complex retrovirus. Therefore, MMTV represents the first complex murine retrovirus (52, 53). Some endogenous betaretroviruses have also been discovered to express a *trans*-acting accessory protein that facilitates the nuclear export of their incompletely spliced transcripts. For instance, the human endogenous retrovirus K (HERV-K) encodes the Rev homolog Rec (54).

1.4 Aim of the study

Numerous epitranscriptional modifications are present in cellular mRNA. The most common modification - the methylation on the N6-Adenosines (m6A)- was proposed to influence the translation, splicing efficiencies, stability, and nuclear export of mRNAs. The presence of m6A on the viral RNAs were reported already several years ago. But only recently, the effect on the virus infectivity was described. It remains to be determined which step of the virus life cycle is affected by the m6A. This project will focus on the effect of m6A modification on the mouse mammary tumor virus (MMTV) mRNA. By knocking out the methyl transferase METTL3, the viral RNA will lack methylations. We hypothesize that the lack of methylation will significantly affect the export of viral RNA into the cytoplasm. This will lead to a reduced viral particle production and loss of infectivity.

Furthermore, cells lacking METTL3 will be used to determine the effect of methylation on nuclear RNA export. This will be done by using a GFP-based nuclear export assay previously established in the laboratory. In this assay, we will test the methylation-dependent activity of tree export elements: 1) the Rev-response element from HIV-1 (RRE, in conjunction with the trans-acting factor Rev), 2) the constitutive transport element (CTE) from Mason-Pfizer monkey virus (MPMV) and 3) a novel cis-acting RNA element, derived from the 5’ end of MMTV env mRNA, MPPE. We hypothesize that the lack of methylation will significantly affect the export of mRNA. This will lead to reduced eGFP production.

With this we will be able to determine whether m6A methylation influence the mRNA export.

2 MATERIAL AND METHODS

2.1 Plasmid construction

2.1.1 pLentiCRISPRv2 with different single guide RNA

To create a knockout in different cell types, lentiviral vectors were used. The vectors were produced using the LentiCRISPRv2 plasmid with a distinct single guide RNA (sgRNA). They delivered the cas9 gene and template for sgRNA to produce the Cas9 ribonucleoprotein complexes (RNPs) in the target cells. The LentiCRISPRv2 plasmid was constructed in the Zhang's laboratory and used together with an sgRNA library (GeCKO) targeting all genes in the human genome. The lentiviral transfer vector contains two expression cassettes. The first for the expression of Cas9 form Streptococcus pyogenes (SpCas9) and the second to produce sgRNA. The 20 nucleotides-long guide sequence of the sgRNA can be cloned upstream of the sgRNA backbone sequence. The plasmid can be digested by BsmBI to create sticky ends for two annealed sgRNA oligos. The ligation was accomplished according to the provided protocol. The guide sequences of sgRNAs were designed by S. Indik. The used guide sequences are listed in Table 1.

For selection of transfected cells, the LentiCRISPRv2 plasmid contains a puromycin acetyltransferase gene conferring resistance to puromycin to transduced cells.

2.1.2 Construction of inducible METTL3 expression plasmids pCMVt53CuO-Mettl3-Hygro

To create the inducible Mettl3 expression plasmids we used a pCMVt53CuO_Cas9 plasmid created by S. Indik. The plasmid contains an inducible promoter CMVt. It is a dual response promoter consisting of combined Tet-ON and Cumate-off systems. The Tet-On inducible portion containing a tetracycline (tet)-responsive element (TRE). The TRE carries seven repeats of the tetracycline operator sequence upstream of a minimal CMV promoter. This portion is only activated when the corresponding transactivator (rtTA3) binds to the TRE. As

activator, we used a tetracycline derivate, doxycycline, that facilitates the binding of rtTA3 to TRE.

For the Cumate Switch system, the repressor protein (CymR) binds to a single operator sequence (CuO) positioned downstream of the CMV TATA box and hinders transcription. After addition of the chemical cumate, the repressor is unable to bind to the operator and transcription takes place.

The CuO operator sequence was introduced to the parental plasmid by a long-template PCR with the primers RRE_F_Nhe and CuO_R_Xba (contains the CuO operator sequecne), which add XbaI and NheI restriction sites. The *Mettl3* gene was amplified from cDNA of HEK293T cells. The primers for *Mettl3* amplification were: Mettl3_F_Xba and Mettl3_R_Nhe. They also add the XbaI and NheI restriction sites at the ends of the amplicon.

The novel pCMVt53CuO plasmid and *Mettl3* open reading frame-–containing amplicon were digested with XbaI and NheI enzymes.

For ligation we useda ratio of 1:3 (vector:insert). The total DNA amount was 110ng. Ligation was carried out with the T4 DNA ligase for one hour at room temperature. The resulting plasmid was named pCMVT53CuO_Mettl3.

To allow selection of cells containing the Mettl3-expression plasmid, we cloned an expression cassette containing the hygromycin resistance gene into the plasmid, respectively. The expression cassettes were amplified with the primers PGK_Not_F and SV40_Not_R using plasmid pLenti_rtTA3_hygro respectively, as a template. The pCMVT53CuO_Mettl3 plasmid and the resistance gene-containing amplicons were digested with EcoRI. Ligations of vector and insert was carried out under the same conditions as described above.

Table 1: Primer for plasmid construction

Primer	**Sequence 5'-3'**
Mettl3 F Xba	TCTAGAATGTCGGACACGTGGAGC
Mettl3 R Nhe	GCTAGCTTACAGAGCCATGGCTATGG
RRE F Nhe	GCTAGCGCAGGAGCTTTGTTCCTTGG
CuO R Xba	TCTAGAGGTAACAAACAGACAATCTGGT
PGK Not F	AAAAAAGCGGCCGCTGGAATTCTACCGGGTAGGG
SV40 Not R	AAAAAAGCGGCCGCCGGGATAGCTAGAGCCAGAC
RTE Xba F	AAAAAATCTAGAAGAAATTATGCTGCGTTATGCC

RTE Xba R	AAAAAATCTAGATTAATTGCTGCAAGCAAGCC

2.1.3 Cloning RTE Export Element into the p3C-CMVtCuOeGFP plasmid

A fragment containing the RTE export element was generated by PCR from the genomic DNA obtained from the mouse cell line, Mm5MT, with the primers RTE_Xba_F and RTE_Xba_R. The fragment was cloned into a

p3C-CMVtCuOeGFP-del plasmid constructed by S. Indik. This plasmid contains the GFP expression cassette and nuclear retention signal derived from the HIV-1 proviral sequences. The plasmid lacks any export element. The PCR product and p3C-CMVtCuOeGFP-del plasmid were digested with XbaI. Then, they were ligated overnight at 16 °C using the T4 DNA ligase (NEB). For ligation a total amount of DNA was150 ng and the vector:insert ratio was 1:3. Other reporter plasmids carrying various RNA export elements were previously designed and created by S. Indik.

2.1.4 Cloning of hNXT1 into the pBRY-IRES-Puro Plasmid

To construct a plasmid for the expression of a RNA export factor, Nxt1, we used a plasmid pBRY-mCherry-IRES-Puro and a gBLOCK synthesized by IDT and containing the Nxt1-coding sequences. Both the plasmid and gBLOCK were digested with EcoRI. The digestion removed the mCherry-coding sequences from the plasmid. The resulting long fragment BRY-IRES-Puro was purified from an agarose gel and used for the ligation with the EcoRI-cut gBLOCK. The vector:insert ratio was 1:3 And the ligation was carried out with the T4 DNA ligation kit (NEB) over night at 16 °C.

2.2 E. coli transformation, cultivation and plasmid preparation

50ng of ligation reaction was used to transform the NEB 5-alpha Competent (High Efficiency) E. coli (17 µL, NEB). Transformations were carried out according to the NEB High Efficiency Transformation Protocol as follows. The DNA was mixed with E. coli and incubated for 30 min

on ice. Next, the cells were incubated at 42 °C for 40 seconds and return on ice. After five minutes-long incubation, the bacteria were resuspended in 250 µL of SOC medium (NEB) and incubated at 37 °C for 45 min on an orbital shaker (200 rpm). Following incubation, 100 µL of the bacterial suspension were streaked out on agar plates containing l ampicillin (100 µg/m). The agar plates were incubated at 37 °C overnight. After incubation, single colonies were picked and cultivated overnight at 37 °C in 2 ml of LB medium containing ampicillin (100 µg/ml)

Plasmid preparations (mini-scale) were carried out according an in-house alkaline-lysis protocol with in-house-made buffers. (Buffer 1: 50 mM glucose, 10 mM EDTA and 25 mM Tris-HCl, pH 8.0, 50 µg/ml RNase A; Buffer 2: 0.2 M NaOH, 1 % SDS; Buffer 3: 3 M potassium acetate, 2 M acetic acid). Briefly, the pelleted bacteria were re-suspended in buffer 1 (300 µL). Next, buffer 2 was added (300 µL) and tubes were carefully mixed. After addition of buffer 3, the tubes were inverted ten times to mix the solutions and centrifuged at 13 000 rpm for 20 min (table top centrifuge). Next, the supernatant containing the plasmid DNA was transferred to tubes with isopropanol (650 µL), mixed and centriguged as shown above. The precipitated DNA was washed one time with 70 % ethanol, dried and re-suspended in water. Successful ligation of inserts to plasmids was identified by using distinct restriction enzymes.

The digested plasmids were visualized on a 1 % agarose gel.The DNA mixed with a loading dye and loaded onto the peqGREEN DNA dye-agarose gel. Electrophoresis was carried out in 1x TAE buffer prepared from 50x concentrated stock solution (50X TAE stock solution for one litre of solution contained: 242 g Tris Base. 57.1 mL Glacial Acetic Acid and 100 mL 0.5 M EDTA). Plasmids with the right restriction pattern were prepared in a large quantity. 20 µL of the miniculture was used to inoculate 30 mL of liquid LB medium. The mid-culture was incubated at 37°C overnight.

Bacterial glycerol stocks were prepared by mixing the overnight midi-culture with glycerol at final concentration of 25 % and stored at -80 °C. Plasmids from the midi-culturewere prepared with the innuPREP Plasmid Mini kit 2.0 (Analytic Jena GmbH) according to their provided protocol. Plasmid concentrations were measured with the NanoBlue Plus spectrophotometer (GEHealthcare) at a wavelength of 260 nm.

To verify successful cloning, every plasmid was sent for sequencing (Mix2Seq Kit by Eurofins Genomics, Germany).

2.3 Cell culture

The cell culture work was done under sterile conditions inside a lamina air-flow bench (Nuaire Minnesota,USA). Cells were cultivated in DMEM supplemented with 10 % fetal calf serum. They were split by trypsinization as follows. The medium was removed and cells washed with in-house PBS (phosphate-buffer saline). Next, the cells were incubated in a solution with 0,5 % Trypsin and EDTA. After detaching from the plastic surface, the cells were re-suspended in the culture media. One third of the mixture was left in the culture bottle and culture medium was added.

2.4 Transient Transfection to produce Lentiviral knockout vectors

For transient transfection, 1x10^6 293T cells were seeded each well of a 6 well-plate one day prior transfection. For each well 3,1 µg of total plasmid DNA was added to 200 µL of OPTIMEM and mixed with a transfection reagent DF2 (4,7 µL, in-house). After 15 min incubation, the mixture was added to cells. Plasmid mixture consist of 0,9 µg psPAX2 (lentiviral packaging construct), 0,6 µg pLP2 (helper plasmid), 0,4 µg pHCMVG (VSV-G envelope protein expression construct) and 1,2 µg pLentiCRISPRv2 with different sgRNA (lentiviral transfer vector plasmid).

15 hours after transfection one third of the cell culture medium was exchanged with a fresh cell culture medium to increase virus production. Lentiviral vectors were harvested 48 hours post transfection and stored at -80 °C.

2.5 Transduction of Mm5MT target cells

For transduction with the knock-out lentiviral vectors, target cell, Mm5MT cells, constitutively expressing mouse mammary tumor virus (MMTV), were seeded onto 6 well plates at a density of 5x10^4 cells per well one day prior transduction. For transduction, the medium was completely removed from Mm5MT cells and replaced with 350 µL of viral vector particles-containing supernatant from 293T cells, supplemented with 3 µL (8 µg/ml final concentration)

polybrene. After 6 hours 0,5 mL of fresh cell medium was added. 24 hours post transduction 2 µM dexamethasone to stimulate MMTV virus production. 48 hours post transduction MMTV containing supernatant was harvested.

2.6 Transduction of CrFK target cells with MMTV

For transduction with MMTV produced by Mm5MT cells, target cell, CrFK cells, were seeded onto 6 well plates at a density of 5x10^4 cells per well one day prior transduction. For transduction, the medium was completely removed from CrFK cells and replaced with 350 µL of viral particles-containing supernatant from Mm5MT cells, supplemented with 3 µL (8 µg/ml final concentration) polybrene. After 6 hours 0,5 mL of fresh cell medium was added.

2.7 DNA extraction and PCR of CrFK target cells

36 hours post transduction of CrFK cells with MMTV cell pellet was harvested. A aliquot was centrifuged, and the pellet washed with PBS. For DNA extraction, an inhouse lysis buffer (10mM TrisCl pH 7; 100 mM NaCl; 1 mM EDTA; 0,1 % SDS) with 10 % Proteinase K was used for cell lysis. The cell-pellet was re-suspended in the lysis buffer containing proteinase K and incubated at 55 °C for one hour. Inactivation of the enzyme was performed at 98 °C for 15min. 1 µL of the genomic DNA was used for PCR.

2.8 Transduction of 293CymRrTA3 target cells

For transduction with the knock-out lentiviral vectors, target cells ,293CymRrTA3 cells, constitutively expressing the rtTA3 activator and CymR repressor, were seeded onto 6 well plates at a density of 5x10^4 cells per well one day prior transduction. For transduction, the medium was completely removed from 293CymRrTA3 cells and replaced with 350 µL of viral vector particles-containing supernatant from 293T cells, supplemented with 3 µL (8 µg/mL final concentration) polybrene. After 6 hours 0,5 mL of fresh cell medium was added.

2.9 Transfection of the transduced 293CymRrTA3 target cells

The transduced cells were transfected with eGFP- and nuclear retention signal-containing plasmids containing different RNA export elements (p3C_- CMVtCuOeGFP_export element). The RNA export elements used in this work were: one copy of the prototypic constitutive transport element (CTE) from the Mason-Pfizer monkey virus (CTE1x), three copies of the same sequence (CTE3x), the RNA transport element from the rodent intracisternal A particles (RTE), the Rev-responsive element from human immunodeficiency virus (HIV-1, RRE) and the mouse mammary tumor virus-derived positive post-transcriptional element (MPPE) cloned either in sense or anti-sense orientation (MPPEanti). The RRE-containing plasmid p3C_CMVtCuOeGFP_RRE was transfected to the 293CymRrTA3 together with Rev-expression construct (pRSV-Rev). Rev is the RNA export protein expressed by HIV-1 to promote export of RRE-containing RNAs. The p3C_CMVtCuOeGFP_RRE plasmid (370 ng) was mixed with pRSV-Rev (185 ng) in 100 µL of OPTIMEM. Other RNA export element -containing plasmids were transfected without the pRSV-Rev. To equalize the total DNA amount for all transfections an “empty” plasmid, pUC19 (185 ng), was added where needed. For each transfection reaction 0,8 µL of DF2 transfection reagent was used. After vortexing and incubation for 15min at room temperature, the mixture was applied dropwise onto the cells.

The cells were induced for 24 hours. Next, Doxycycline (100 ng/mL) and Cumate (30 µg/mL) were added and incubated for additional 17 hours. The expression of GFP was measured flow cytometry (FACS) and UV microscopy.

2.10 Transfection of plasmids with export elements together with the NXT1 and NXF1-expression constructs

Transient transfection of 293CymRrtTA3 cells were carried out with the following conditions. 293CymRrTA3 cells were seeded one day prior transfection to a 12 well plate at a density of 1x10^4 cells per well.

Transfection reactions were mixed as follows: to 100 µL of OPTIMEM p3C_CMVtCuOeGFP_export element-containing plasmid (370 ng) and NXT1-expression plasmid (400 ng of) and/or NXF1-expression construct (100 ng). To balance DNA amount the

“empty” plasmid (pUC19) was added where needed. Additionally, 25 ng of pNLXluc was added to every reaction for the luciferase assay that was used to control the transfection efficiency. To DNA (the total amount of 1195 ng) 1,8 µL of transfection reagent, DF2, was applied. After vortexing and the incubation for 15 min at room temperature the mixture was applied dropwise onto the cells.

24 hours post transfection Doxycycline (100 ng/mL) and Cumate (30 µg/mL) was added to cells After additional 17 hours GFP expression was measured by flow cytometry and UV microscopy.

2.11 Determination of knock-out efficiency

For the determination of the knockout rate in the target cells, an aliquot of the cells was taken before FACS analysis. The aliquot was centrifuged, and the pellet washed with PBS. For DNA extraction, an inhouse lysis buffer (10 mM TrisCl pH 7; 100 mM NaCl; 1 mM EDTA; 0,1 % SDS) with 10 % Proteinase K was used for cell lysis. The cell-pellet was re-suspended in the lysis buffer containing proteinase K and incubated at 55 °C for one hour. Inactivation of the enzyme was performed at 98 °C for 15 min. 1 µL of the genomic DNA was used for PCR that amplified the region targeted by Cas9/sgRNA complex.

To estimate the knockout rate, the PCR product was sequenced (Eurofins Genomics). The chromatograms from the Sanger sequencing were used for a deconvolution analysis with the ICE Analysis Program provided on the Synthego Homepage (https://ice.synthego.com/#/).

2.12 Fluorescence microscopy and flow cytometry

For florescence microscopy the Olympus IX70 microscope was used. Pictures were taken with the corresponding CellSense software (Olympus).

For flow cytometry cells were harvested by trypsination and resuspended in PBS with 4% formaldehyde. The cells were filtered through a 100 µm mesh filter (Brückmann, Mönchengaldbach, Germany) to a 5ml FACS tubes with. The samples were analysed with the BD FACSCalibur fluorescence activated cell sorter and the corresponding CellQuest software

(Becton Dickinson, California). In total, 50000 events were counted per sample. To exclude debris and dead cells from the analysis untransfected cells were used for calibration. EGFP expression was detected by a shift in fluorescence intensity in the FL-1 channel.

3 RESULTS

3.1 Selection of suitable sgRNA for Mettl3 knock-out

Gene editing is one of the important tools to study gene function. Recently, the clustered regularly interspaced short palindromic repeats (CRISPR)/ CRISPR associated protein 9 (Cas9) method became one of the most promising techniques in the field of genome editing. This system consists of two major components the Cas9 protein and a single guide RNA (sgRNA). The protein is a DNA endonuclease that uses sgRNA to target DNA region of interest. Cas9 unwinds the foreign DNA and searches for loci that are complementary to the 20 nucleotides-long spacer region of the sgRNA. When the endonuclease detects the complementary sequence located next to a protospacer-adjacent motif (PAM, Cas9 from Streptococcus pyogenes requires NGG sequence), double stranded break is introduced to the targeted locus. During the repair of the cleaved region, which is catalysed by cellular enzymes of the non-homologous end joining (NHEJ) pathway, several nucleotides are often randomly inserted or deleted at the junction site. These indels may change the reading frame of the targeted gene and result in the disruption or alteration of the gene functionality (55). The efficiency and specificity of this process is determined by the single guide RNA. That's why it is important to find highly efficient sgRNAs (56).

Our aim was to knock-out the *Mettl3* gene and determine how the knock-out affects the nuclear export of RNA molecules carrying various RNA export elements. In the first step, we wanted to identify a sgRNA with a high knock-out rate. We designed six sgRNAs targeting the *Mettl3* gene in the human genome (Mettl3_h1, Mettl3_h2, Mettl3_h3, Mettl3_h4, Mettl3_h5, Mettl3_hSY1, Mettl3_hSY2). Moreover, because we wanted to analyse the nuclear export also in cell lines of the feline and murine origin, we also designed six additional sgRNAs targeting the *Mettl3* gene in the feline (Mettl3_cat_SY1, Mettl3_cat_SY3, Mettl3_cat_SY4) and murine (Mettl3_M1, Mettl3_M2, Mettl3_M3,) genome. To test the Mettl3 disruption efficiency of the sgRNAs, we used a previously described lentivector-based system (57). The lentivector carries the Cas9 protein and expresses sgRNA in the targeted cells. The system efficiently disrupts genes in a variety of cell types, including the primary cells. In addition, as the system does not overexpress the Cas9 protein, it is less prone to off-targeting. We transduced the human (HEK293T), cat (CrFK) and mouse (Mm5Mt) cell lines with lentiviral vectors containing various

sgRNA coding sequences. Two days after transduction, the cells were harvested, and the genomic DNA extracted from the cells. The specific regions containing the targeted sites were amplified by PCR and successful amplification was verified by agarose gel electrophoresis. Next, the PCR products were sent for sequencing (Eurofins Genomics, https://eurofinsgenomics.eu/). The Sanger sequencing chromatograms were first manually inspected for the presence of a "mixed" sequence downstream of the targeted site, which indicates a successful introduction of the indels to the loci. Next, the chromatograms were used for *in silico* analysis that can precisely determine the frequency of indel formation as well as the proportion of sequences carrying the gene-disrupting mutation (knock-out (KO) score). For the in silico analysis, we used the ICE (Inference of CRISPR edits) analysis programme provided by the Synthego (https://ice.synthego.com/)). The software aligns the wild type DNA target site (obtained from mock transduced cells) with the knock-out region (DNA extracted from transduced cells) and calculates the rates. The tested sgRNAs and the determined knock-out score is shown in *Table 2.*

***Table 2: sgRNA with corresponding sequence and knock-out efficiency**.*

Gene	**Species**	**guide Name**	**Sequence 5'-3'**	**KO score by Synthego**
Mettl3	human	Mettl3_h1	TAGGCACTGGGCTGTCACTAngg	47%
Mettl3	human	Mettl3_h2	AGCATCAGTGGGCAATGTTAngg	20%
Mettl3	human	Mettl3_h4	AGACTAGGATGTCGGACACGngg	85%
Mettl3	human	Mettl3_h5	GGACACGTGGAGTCTATCCngg	86%
Mettl3	human	Mettl3_hSY1	TCTCTTCATTCTTAGATCTAngg	67%
Mettl3	human	Mettl3_hSY2	CTTAGATCTACGGAATCCAGngg	2%
Mettl3	cat	Mettl3_cat_SY1	TCCAGATCTACGAAATCCAGngg	73%
Mettl3	cat	Mettl3_cat_SY3	GGACTGTCACTGCGGAAGGTngg	58%
Mettl3	cat	Mettl3_cat_SY4	TGGACTGTCACTGCGGAAGGngg	71%
Mettl3	mouse	Mettl3_M1	GGACACGTGGAGCTCTATCCngg	87%
Mettl3	mouse	Mettl3_M2	CGCTTCGCGAGAGATTGCAGngg	0%
Mettl3	mouse	Mettl3_M3	ACTATCACTACGGAAGGTTGngg	30%

We detected at least one highly efficient single guide RNA for each species. The highest KO score in the human cells was obtained for the sgRNA Mettl3_h5 (86%), see Figure 6. For the

Mettl3_h4 sgRNA, was the KO efficiency only moderately reduced (85 %) in comparison to the highest scoring sgRNA. For the mouse genome, we determined the highest KO score for the sgRNA Mettl3_M1 (87 %), see Figure 4. The sgRNA Mettl3_Cat_SY1 showed the best performance (73 %) in the cat genome, see Figure 5.

A closer look at the KO caused by CRISPR/Cas9 system, revealed that the sgRNA Mettl3_M1 (*Figure 4*) in murine cells tended to cause a deletion of four bases (frequency of 22 %) and an insertion of one base pair (found in 37 % of sequences). Other deletions have a lower incidence compared to the most prevalent ones . When all indels were combined, the overall KO rate was 87 %. In feline cells, the most common indels for sgRNA Mettl3_cat_SY1 (Figure 5) were plus and minus one base pair, with a frequency of 15 % and 17 %, respectively. The overall KO rate for the Mettl3_cat_SY1 sgRNA was 73 %. Finally, in human HEK293T cells, the Mettl3_h5 sgRNA mainly caused an insertion of one base pair (fond in 12 % of sequences) and a deletion of four base pairs (found in 17 % of sequences). Both mutations result in a frame shift. Deletions of ten and eleven base pairs were also common (with frequency of 11 % and 8 %, respectively) (Figure 6).

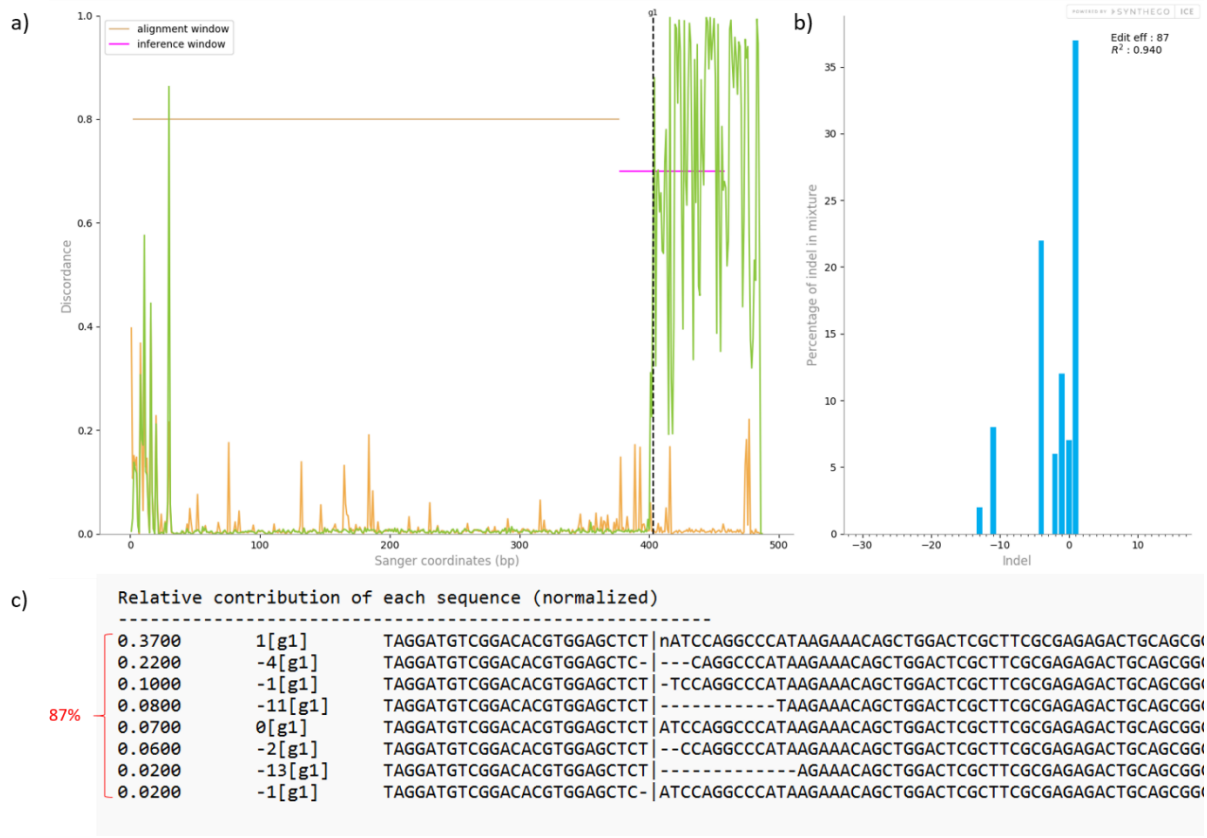

Figure 4: ICE analysis result for sgRNA Mettl3_M1: Result of the ICE analysis of Synthego with sgRNA Mettl3_M1 in Mm5MT cells. a) Shows the alignment window and inference window. With the alignment window showing the region where control sequence and target sequence align. The inference window represents the region with indel (insertion and deletion) and therefore control and target sequences can't align anymore. Which starts in the case of sgRNA Mettl3_M1 at about 400bp into the sequenced region of the *Mettl3* gene. b) Gives an overview of the percentage of indel's for the *Mettl3* KO in form of a bar diagram. With 37 % and 22 % giving the highest percentage of indel's. c) The left column gives the frequency of each indel. The second column gives the type of indel mutation with "-" for deletion and "+" for insertion. In the last column the indel is visible within the sequence. The most common indels for this specific sgRNA are an insert of one base with a frequency of 37% and a deletion of four bases with a frequency of 22%, both causing a frameshift and therefore a non-functional *Mettl3* gene.

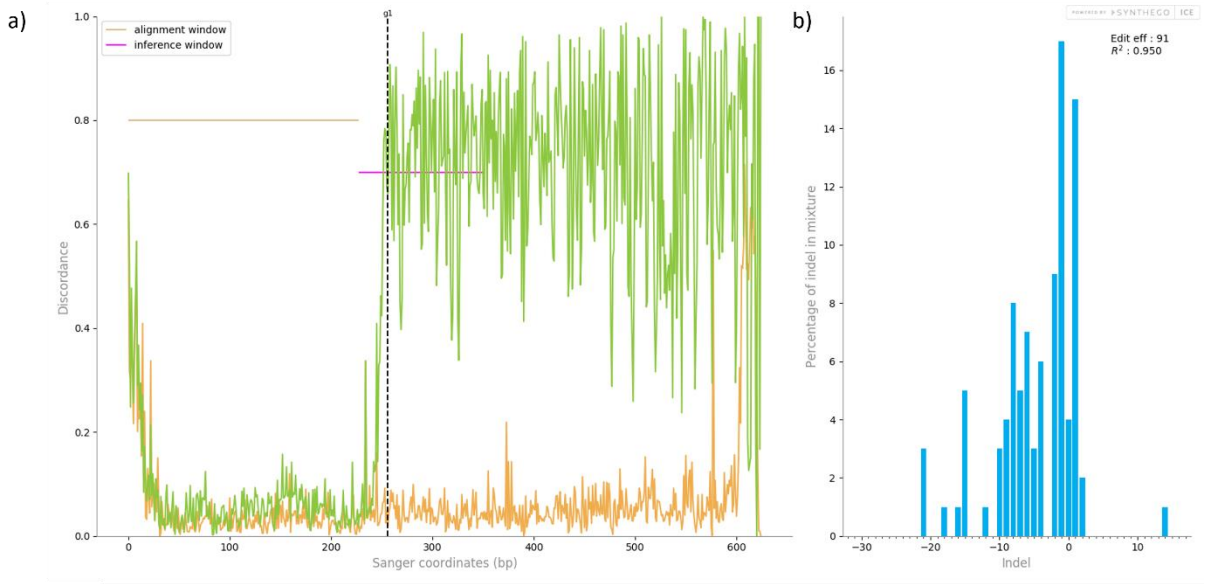

c)

Relative contribution of each sequence (normalized)

0.1700	-1[g1]	TCTTCATTCCCAGATCTACGAAATC|-AGAGGCAGCACTGTCTCCCACCTTCCGCAGTGACAGTCCAGTGCCTGCTGCACCCACTTCTGGTGGCCCTAAGC
0.1500	1[g1]	TCTTCATTCCCAGATCTACGAAATC|nCAGAGGCAGCACTGTCTCCCACCTTCCGCAGTGACAGTCCAGTGCCTGCTGCACCCACTTCTGGTGGCCCTAAG
0.0800	-8[g1]	TCTTCATTCCCAGATCTACGAAATC|--------GCACTGTCTCCCACCTTCCGCAGTGACAGTCCAGTGCCTGCTGCACCCACTTCTGGTGGCCCTAAGC
0.0600	-6[g1]	TCTTCATTCCCAGATCTAC------|CAGAGGCAGCACTGTCTCCCACCTTCCGCAGTGACAGTCCAGTGCCTGCTGCACCCACTTCTGGTGGCCCTAAGC
0.0500	-2[g1]	TCTTCATTCCCAGATCTACGAAAT-|-AGAGGCAGCACTGTCTCCCACCTTCCGCAGTGACAGTCCAGTGCCTGCTGCACCCACTTCTGGTGGCCCTAAGC
0.0400	0[g1]	TCTTCATTCCCAGATCTACGAAATC|CAGAGGCAGCACTGTCTCCCACCTTCCGCAGTGACAGTCCAGTGCCTGCTGCACCCACTTCTGGTGGCCCTAAGC
0.0400	-2[g1]	TCTTCATTCCCAGATCTACGAAATC|--GAGGCAGCACTGTCTCCCACCTTCCGCAGTGACAGTCCAGTGCCTGCTGCACCCACTTCTGGTGGCCCTAAGC
0.0400	-15[g1]	TCTTCATTCCCAGATCTACGAAATC|---------------CTCCCACCTTCCGCAGTGACAGTCCAGTGCCTGCTGCACCCACTTCTGGTGGCCCTAAGC
0.0400	-4[g1]	TCTTCATTCCCAGATCTACGA----|CAGAGGCAGCACTGTCTCCCACCTTCCGCAGTGACAGTCCAGTGCCTGCTGCACCCACTTCTGGTGGCCCTAAGC
0.0300	-5[g1]	TCTTCATTCCCAGATCTACGAA---|--GAGGCAGCACTGTCTCCCACCTTCCGCAGTGACAGTCCAGTGCCTGCTGCACCCACTTCTGGTGGCCCTAAGC
0.0300	-7[g1]	TCTTCATTCCCAGATCTACGAA---|----GGCAGCACTGTCTCCCACCTTCCGCAGTGACAGTCCAGTGCCTGCTGCACCCACTTCTGGTGGCCCTAAGC
0.0300	-9[g1]	TCTTCATTCCCAGATCTACGAA---|------CAGCACTGTCTCCCACCTTCCGCAGTGACAGTCCAGTGCCTGCTGCACCCACTTCTGGTGGCCCTAAGC
0.0300	-10[g1]	TCTTCATTCCCAGATCTACGA----|------CAGCACTGTCTCCCACCTTCCGCAGTGACAGTCCAGTGCCTGCTGCACCCACTTCTGGTGGCCCTAAGC
0.0300	-21[g1]	TCTTCATTCCCAGATCTAC------|---------------CTCCCACCTTCCGCAGTGACAGTCCAGTGCCTGCTGCACCCACTTCTGGTGGCCCTAAGC
0.0200	-4[g1]	TCTTCATTCCCAGATCTACGAAA--|--GAGGCAGCACTGTCTCCCACCTTCCGCAGTGACAGTCCAGTGCCTGCTGCACCCACTTCTGGTGGCCCTAAGC
0.0200	-7[g1]	TCTTCATTCCCAGATCTACGAAA--|-----GCAGCACTGTCTCCCACCTTCCGCAGTGACAGTCCAGTGCCTGCTGCACCCACTTCTGGTGGCCCTAAGC
0.0200	2[g1]	TCTTCATTCCCAGATCTACGAAATC|nnCAGAGGCAGCACTGTCTCCCACCTTCCGCAGTGACAGTCCAGTGCCTGCTGCACCCACTTCTGGTGGCCCTAA
0.0100	-6[g1]	TCTTCATTCCCAGATCTACGAAATC|------CAGCACTGTCTCCCACCTTCCGCAGTGACAGTCCAGTGCCTGCTGCACCCACTTCTGGTGGCCCTAAGC
0.0100	-9[g1]	TCTTCATTCCCAGATCTACGAAATC|---------CACTGTCTCCCACCTTCCGCAGTGACAGTCCAGTGCCTGCTGCACCCACTTCTGGTGGCCCTAAGC
0.0100	-16[g1]	TCTTCATTCCCAGATCTACGAA---|-------------GTCTCCCACCTTCCGCAGTGACAGTCCAGTGCCTGCTGCACCCACTTCTGGTGGCCCTAAGC
0.0100	-18[g1]	TCTTCATTCCCAGATCTACGAA---|---------------CTCCCACCTTCCGCAGTGACAGTCCAGTGCCTGCTGCACCCACTTCTGGTGGCCCTAAGC
0.0100	-12[g1]	TCTTCATTCCCAGATCTAC------|------CAGCACTGTCTCCCACCTTCCGCAGTGACAGTCCAGTGCCTGCTGCACCCACTTCTGGTGGCCCTAAGC
0.0100	-15[g1]	TCTTCATTCCCAGATCTAC------|---------CACTGTCTCCCACCTTCCGCAGTGACAGTCCAGTGCCTGCTGCACCCACTTCTGGTGGCCCTAAGC
0.0100	14[g1]	TCTTCATTCCCAGATCTACGAAATC|nnnnnnnnnnnnnnCAGAGGCAGCACTGTCTCCCACCTTCCGCAGTGACAGTCCAGTGCCTGCTGCACCCACTTC

73%

***Figure 5: ICE analysis result for sgRNA Mettl3 CatSY1*:** Result of the ICE analysis of Synthego with sgRNA Mettl3_cat_SY1 in CrFK cells. a) Shows the alignment window and inference window. With the alignment window showing the region where control sequence and target sequence align. The inference window represents the region with indel (insertion and deletion) and therefore control and target sequences can't align anymore. Which starts in the case of sgRNA Mettl3 _cat_SY1 at about 250bp into the sequenced region of Mettl3. b) Gives an overview of the percentage of indel in the mixture in form of a bar diagram. With 17 % and 15 % giving the highest percentage of indel's. c) The left column gives the frequency of each indel. The second column gives the type of indel mutation with "-" for deletion and "+" for insertion. In the last column the indel is visible within the sequence. The most common indels for this specific sgRNA are a deletion of one base with a frequency of 17% and an insertion of one base with 15%, both causing a frameshift and therefore a non-functional Mettl3 gene.

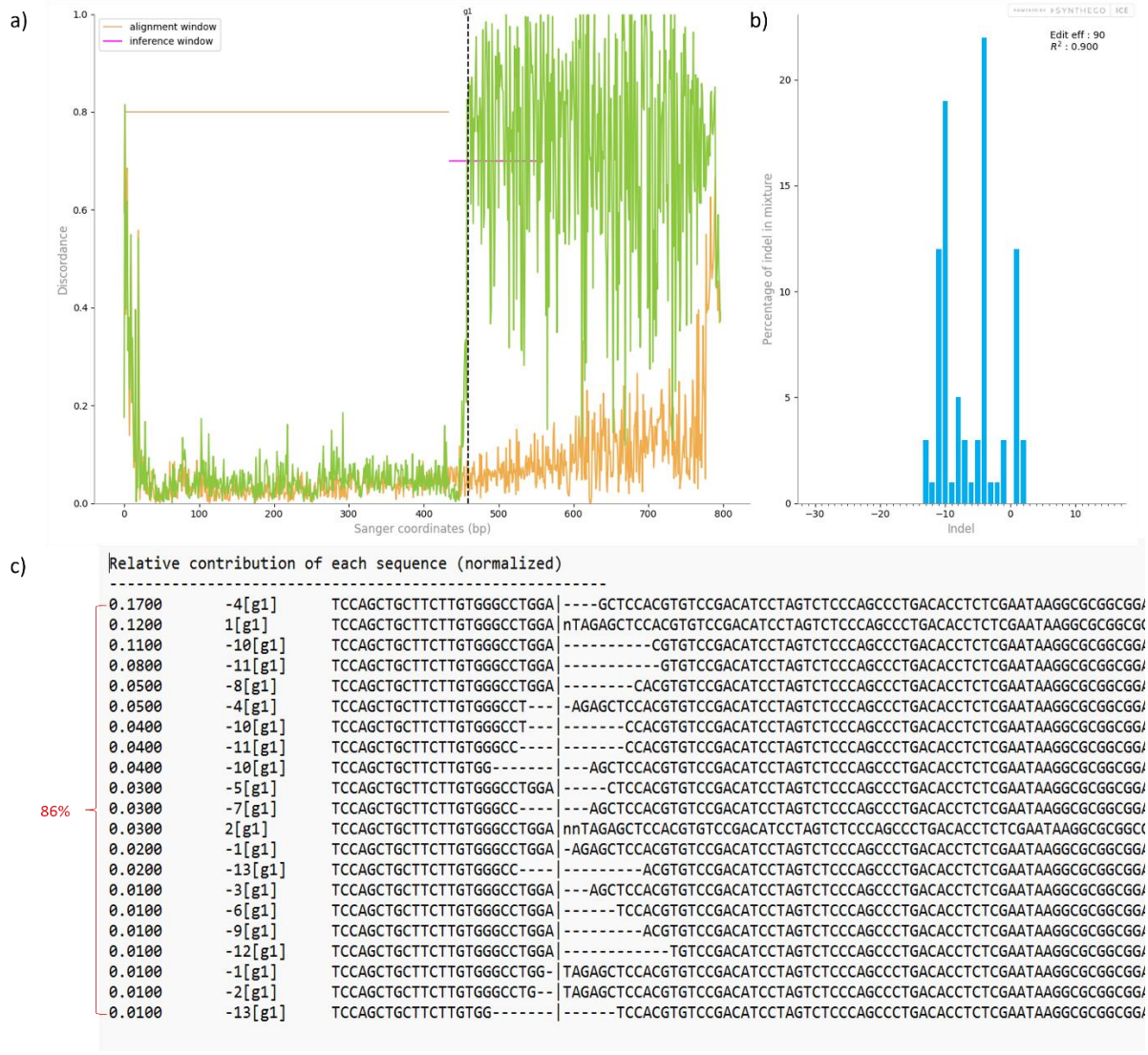

Figure 6: ICE analysis result for sgRNA Mettl3 h5: Result of the ICE analysis of Synthego with sgRNA Mettl3 h5 in HEK293 cells. a) Shows the alignment window and inference window. With the alignment window showing the region where control sequence and target sequence align. The inference window represents the region with indel (insertion and deletion) and therefore control and target sequences can't align anymore. Which starts in the case of sgRNA Mettl3_h5 at about 450bp into the sequenced region of *Mettl3*. b) Gives an overview of the percentage of indel in the mixture in form of a bar diagram. With 17 % and 12 % giving the highest percentage of indel's. c) The left column gives the frequency of each indel. The second column gives the type of indel mutation with "-" for deletion and "+" for insertion. In the last column, the indel is visible within the sequence. The most common indels for this specific sgRNA are a deletion of four bases with a frequency of 17 % and an insertion of one base with 12 %, both causing a frameshift and therefore non-functional Mettl3 gen. Additional important deletions are minus ten and minus eleven base pairs with 11 % and 8 %

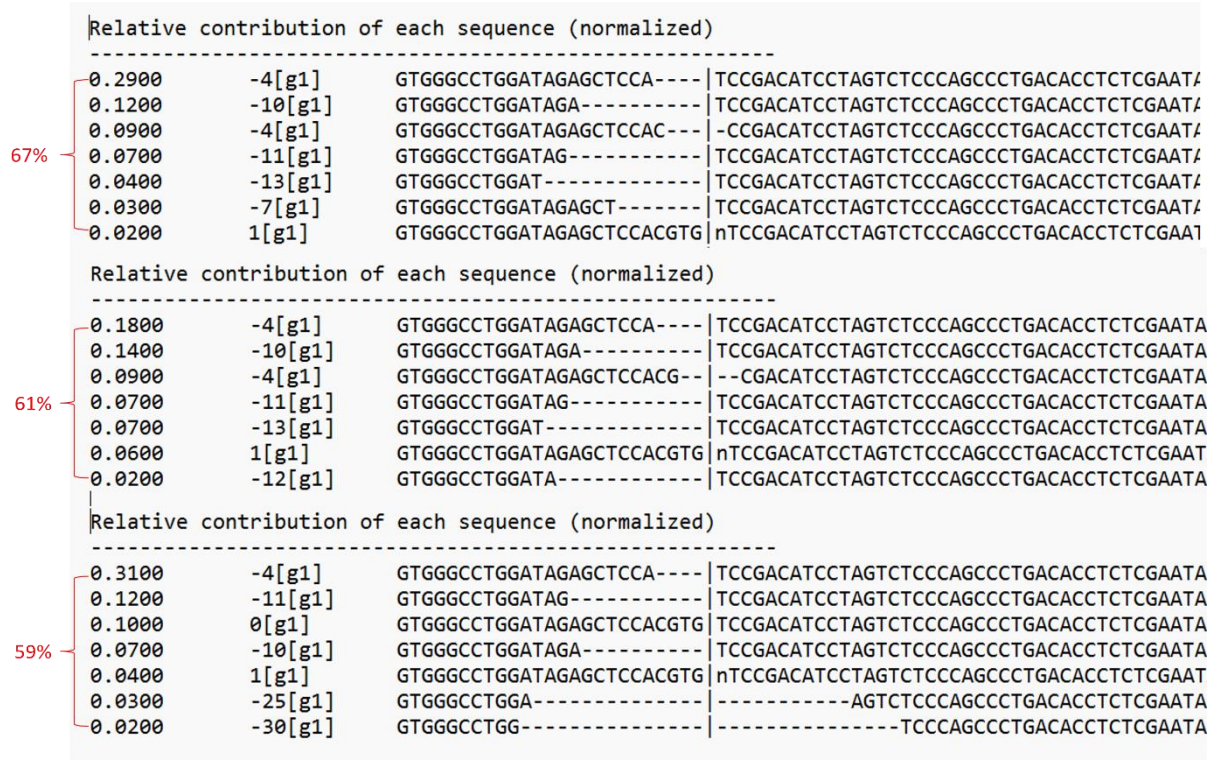

***Figure 7: ICE Result of Mettl3_h5*:** This figure shows the knock-out rate with the most prevalent indels for sgRNA Mettl3 h5. On the left side the KO rate for each individual KO, from which the data were used below, can be seen. The KO score is between 59% and 67%. The first column gives the percentage of each individual indel, the following column displays the specific indel. With the most common deletion of four bases and equally important deletion of minus ten and minus eleven base pairs. The last column gives the position of the indel within the sequence.

For further experiments, we decided to continue with the human HEK293T cells and mouse Mm5MT cells. For human cells, we decided to go on with the most efficient sgRNA is called Mettl3_h5. As a negative control, we decided to use the sgRNA Mettl3_hSY2 that showed the lowest KO rate of 2 %. First, we wanted to determine if the KO efficiencies are reproducible. For every repeat of the experiment, the KO rate was determined for both guide RNAs. The determined knock-out rate for the sgRNA Mettl3_h5 was lower than the previously determined KO rate (86 %). An average KO rate for sgRNA Mettl3_h5 was 62 % (Figure 7). The most prevalent indel was the deletion of four base pairs with an average frequency of 38 %. Furthermore, deletions of ten and eleven base pairs were detected with a frequency of 12 % and 7 %(Figure 8). The knock-out rate for sgRNA Mettl3_hSY2 was 0 % in every repeat of the experiment (Data not shown).

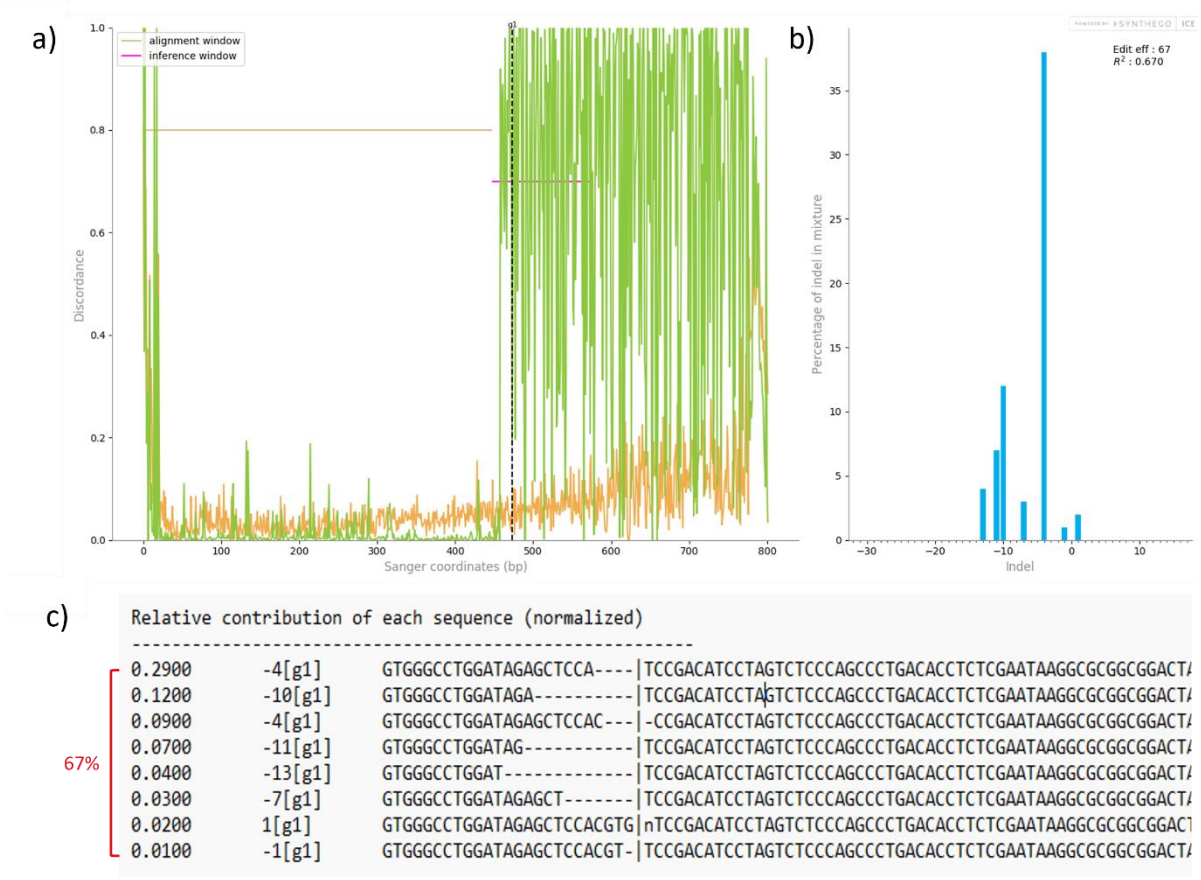

Figure 8: ICE analysis result for sgRNA Mettl3 h5 67 % knock-out rate: a) shows the alignment window and inference window. With the alignment windows showing the region where control sequence and target sequence align. The inference window represents the region with indel and therefore control and target sequences can't align anymore. b) gives an overview of the percentage of indel in the mixture. c) the left column gives the frequency of each indel. The second column gives the type of indel mutation with "-" for deletion and "+" for insertion. In the last column the indel is visible within the sequence.

We observed a similar result with the sgRNA Mettl3_M1. Also in this case the KO rate was lower in the repeated transductions compared to the initial experiment. The average KO-rate was reduced from 87 % to 63 %. The most prevalent indel for this sgRNA was an insertion of one base pair. In two biological replicates, the 1nt deletion was observed in 37 % and 22 % of sequences, respectively. The Mettl3_M2 sgRNA showed no KO. Therefore, we will use this sgRNA as a control.,

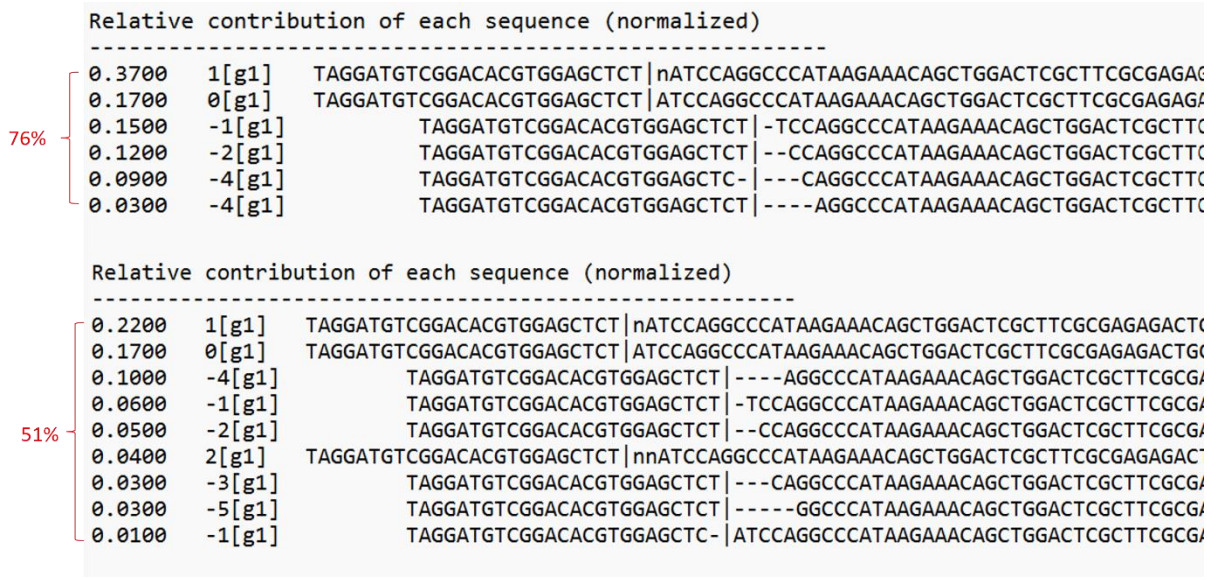

Figure 9: ICE Result of Mettl3_M1: This figure shows the knock-out rate with the most prevalent indels for sgRNA Mettl3 M1. On the left side the KO rate for each individual KO, from which the data were used, can be seen. The KO score is on average 63,5% The first column gives the percentage of each individual indel, the following column displays the specific indel. With the most common deletion of four bases and equally important deletion of minus ten and minus eleven base pairs. The last column gives the position of the indel within the sequence

3.2 Influence of *Mettl3* knockout on MMTV virus production in Mm5MT cells

Mm5MT cells is a mouse cell line chronically infected with mouse mammary tumor virus (MMTV). The cells produce MMTV after incubation of the cells in dexamethasone-containing medium that induces the virus production by inducing the virus promoter. After determination of the best performing sgRNA for disruption of the *Mettl3* gene in Mm5MT cells, we used the cells transduced either with the lentivector expressing Mettl3_M1 sgRNA the control lentivector producing the Mettl3_M2 sgRNA to produce MMTV virus. The viruses were then used to infect the permissive feline CrFK cell line. As part of the retroviral life cycle, the reverse transcribed DNA of MMTV integrates into the genome of the target CrFK cells. Thus, we could use a virus-specific semi-quantitative PCR to detect if MMTV was produced in the KO and control cells, infected the feline target cells and finally integrated into the host feline genome.

As shown in Figure 10, CrFK cells infected with MMTV produced from untreated Mm5MT cells show a PCR product of the expected size, indicating successful infection and integration of the

MMTV virus into the feline genome (Figure 10 position 12-13, two independent biological replicates). Without infection no PCR product was detected in the lysates of CrFK cells (Figure 10, lane 14). At lane eight and nine are PCR products generated from CrFK cells were infected with MMTV, which was produced by Mm5MT cells previously transduced with the sgRNA Mettl3_M1 that induced the *Mettl3* knockout. Lanes 10 and 11 show the PCR products produced from lysates of CrFK cells infected with MMTV produced by Mm5MT cells previously transduced with sgRNA Mettl3_M2, which does not knock out *Mettl3* gene. Position 8 and 9 show the amplicons from CrFK cells infected with MMTV produced from Mm5MT cells carrying crippled Mettl3 gene. There seems to be no difference in the intensities of the PCR products. Thus, we concluded that it appears that disruption of the Mettl3 gene has no effect on the infectivity of MMTV.

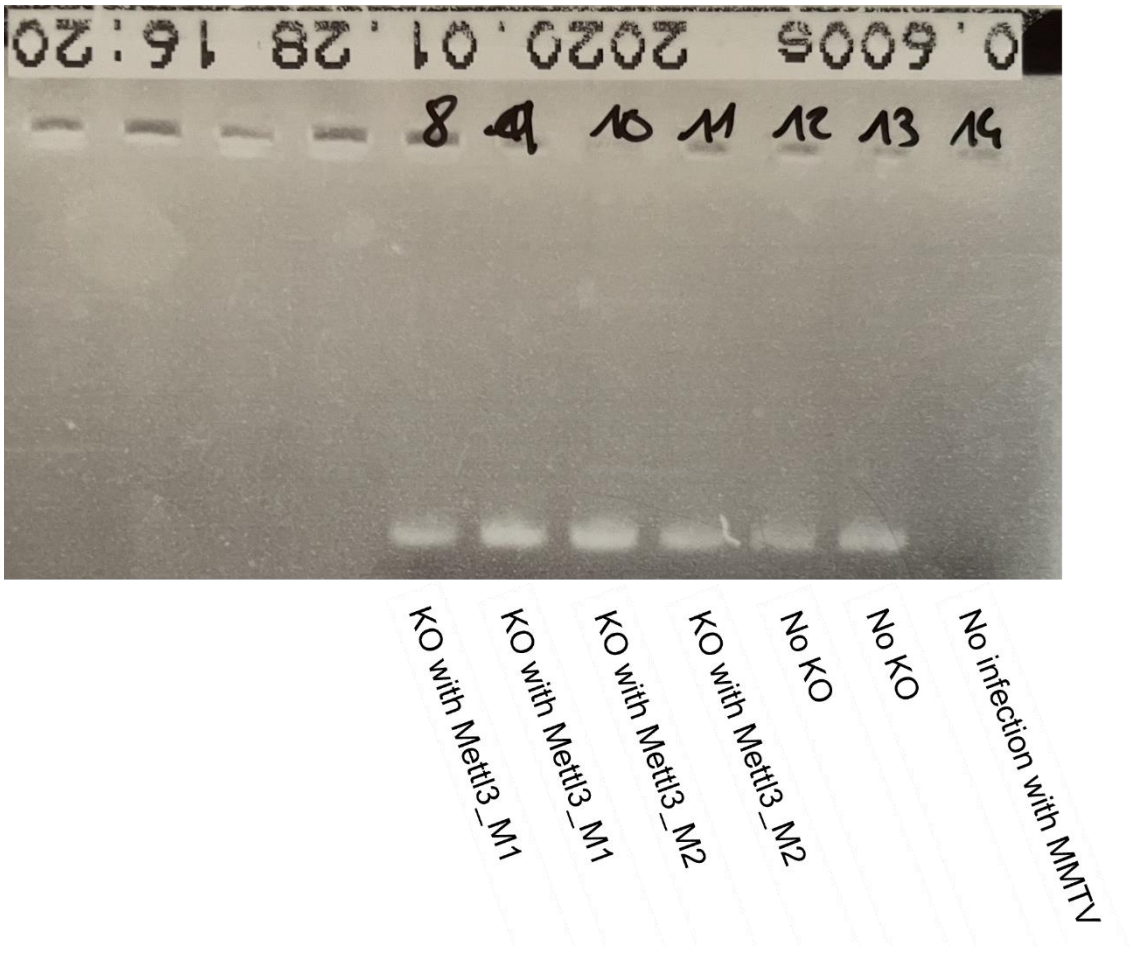

Figure 10: PCR product of CrFK cells infected with MMTV*:* Lanes 8 and 9 show CrFK cells infected with MMTV produced by Mm5MT cells having a *Mettl3* knockout, caused by sgRNA Mettl3_M1. Lanes 10 and 11 show CrFK infected with MMVT produced by Mm5MT cells having a functional *Mettl3* gen

but transduced with a mock knockout. Lanes 12 and 13 show CrFK cells infected with MMTV produced by normal Mm5MT cells. Lane 14 show PCR with CrFK cells which aren't infected with MMTV, resulting in no PCR product.

3.3 Influence of *Mettl3* knock-out on the eGFP expression from RNA export reporter construct

3.3.1 eGFP expression in Mettl3 KO vs no KO

After determining the best performing sgRNA for the disruption of the *Mettl3* gene in the human genome, we could start to test whether the knockout of *Mettl3* gene will have an effect on the eGFP expression from our reporter system carrying various RNA export elements. The reporter expression construct was previously developed by a MSc student Bernhard Willdom in the Indik's group. The construct named p3C-d-CMVt.CuO.eGFPpA contains an inducible promoter that drives the expression of eGFP in the presence of doxycycline and/or cumate. Furthermore, the construct carries the nuclear retention signal from HIV-1, which prevents eGFP expression in the absence of an RNA export element. A number of cis-acting nuclear export elements have been identified in the mRNA molecules expressed from retroviral proviral DNA. It includes the constitutive export element (CTE) identified in the mRNA produced from the Mason-Pfizer monkey virus (MPMV) proviral sequences (33). Cis-acting element detected in rodent intra-cisternal A-particle retroelements (RTE) (39), a novel cis-acting RNA export element detected in the env mRNA derived from the mouse mammary tumor virus (MPPE, unpublished data); and finally an RNA segment from the HIV-1 virus (Rev responsive element, RRE) that promotes RNA nuclear export in the presence of viral accessory protein, Rev (41). Whereas the RRE/Rev facilitates the nuclear export via the CRM1 pathway, the CTE and RTE promote cytoplasmic localization via the canonical, Nxf1-dependent, mRNA export pathway (58, 59).

In total, seven distinct p3C-d-CMVt.CuO.eGFPpA-based plasmids were used. Six plasmids contain the following RNA export elements: one copy of CTE (p3C-CMVt10CuO.eGFPpA-CTE), three copies of CTE (p3C-CMVt10CuO.eGFPpA-3xCTE), RTE p3C-CMVt10CuO.eGFPpA-RTE, RRE from HIV-1 p3C-CMVt10CuO.eGFPpA-RRE , and finally MPPE that was cloned in the sense and in antisense orientation to the plasmid backbone

resulting in plasmids named p3C-CMVt10CuO.eGFPpA-MPPE and p3C-CMVt10CuO.eGFPpA-MPPEanti. The seventh reporter plasmid, p3C-CMVt10CuOeGFPpA-del, which lacks any cis-acting element, served as a negative control.

To determine whether the disruption of the *Mettl3* gene has an effect on the mRNA export efficiency, we transduced the human cells with the knock-out lentivector carrying Cas9 protein and the coding region for the highest-scoring sgRNA (Mettl3_h5). Two days after transduction, the cells were transfected with plasmids carrying various RNA export elements. We used 0.5 µg of plasmid DNA that was mixed with 0,76 µL of a polyethylenimine (PEI)-based transfection reagent (DF2). The plasmid p3C-CMVt10CuO.eGFPpA-RRE was co-transfected with the Rev expression construct. The target cells, 293CymRrtTA3, constitutively express a cumate repressor (CymR) and a reverse tetracycline activator (rtTA3) that allows the initiation of transcription of the eGFP gene by supplementing doxycycline and/or cumate into the cell culture media.

Normalization was performed to cells transfected with a plasmid which constitutively expresses eGFP (pCMVeGFP). The statistical significance of differences between eGFP expression levels obtained from no Mettl3 knock-out and Mettl3 knock-out cells for each reporter element was calculated with an unpaired t-test.

The percentage of eGFP positive cells transfected with p3C-CMVt10CuOeGFPpA-del, which is the control group, was about 18 %. The highest percentage of eGFP positive cells was found in p3C-CMVt10CuOeGFPpA-MPPEanti transfected cells having the *Mettl3* knock-out, with an average value of 24.5 %. When comparing the percentage of eGFP positive cells in the *Mettl3* knock-out vs no *Mellt3* knock-out groups, we observed a tendency for a higher amount of eGFP-positive cells in the no *Mettl3* knock-out group However, this tendency was never statistically significant. There are exceptions where the *Mettl3* knock-out group has more eGFP positive cells compared to the no knock-out group. For example, the p3C-CMVt10CuOeGFPpA-MPPEanti transfected cells, or the cells co-transfected with p3C-CMVt10CuO.eGFPpA-RRE plasmid and Rev expression construct. Again, there was no significant difference to the no knock-out group. Having a closer look at the export element p3C-CMVt10CuO.eGFPpA-MPPE and its counterpart p3C-CMVt10CuO.eGFPpA-MPPEanti. All four groups (MPPE/Mettl3 knock-out and no knock-out and MPPEanti/Mettl3 with and

without knock-out) showed a higher percentage of eGFP positive cells compared to the other export elements or control group. (see Figure 11 and Figure 13).

Beside the percentages of eGFP positive cells, we also monitored the MFI (Mean Fluorescence Intensity). Here, p3C-CMVt10CuO.eGFPpA-MPPE shows a statistically significantly stronger MFI signal than p3C-CMVt10CuO.eGFPpA-MPPEanti. Same applies to p3C-CMVt10CuO.eGFPpA-RRE + rev (higher signal) and p3C-CMVt10CuO.eGFPpA-RRE without rev (lower signal). A significant difference in the MFI between export elements can be observed in p3C-CMVt10CuO.eGFPpA-CTE1x and p3C-CMVt10CuO.eGFPpA-CTE3x (data not shown). Importantly, there is no significant difference within knock-out group and control group in either of the export elements. The highest MFI are observed for p3C-CMVt10CuOeGFPpA-CTE3x, p3C-CMVt10CuOeGFPpA-RRE+rev and p3C-CMVt10CuOeGFPpA-MPPE plasmids (see Figure 12 and Figure 13).

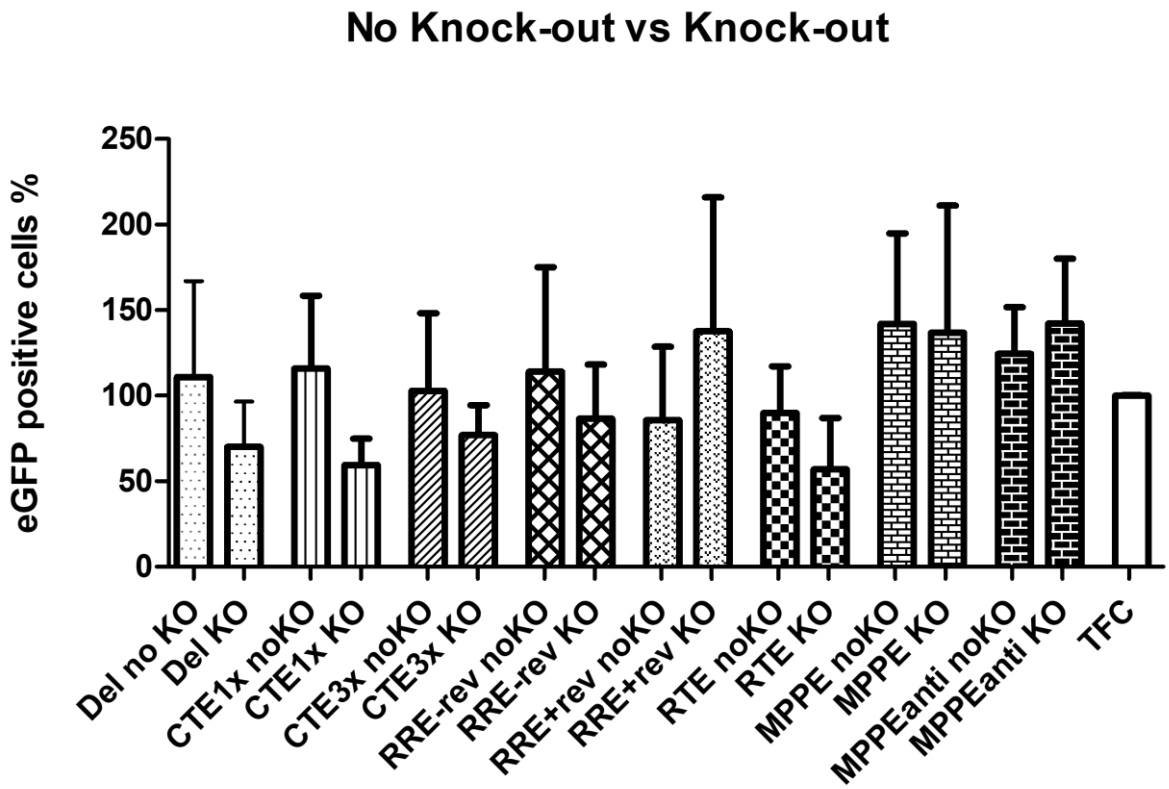

Figure 11: eGFP positive cell count comparing no knock-out with knockout of different p3C-CMVt10CuOeGFPpA reporter elements: eGFP positive cells were normalized to transfection control (TFC) which was transfected with a constitutively expressing eGFP plasmid (pCMV-eGFP). No

significant difference between no knock-out and knock-out group can be detected. Significance differences between the no knock-out group and knock-out group, within each reporter system, was calculated with a two-tailed, unpaired t-test for equal or unequal variances, depending on the outcome of previously performed F-test for equality of variances. *: p=<0.05, **: p=<0.01. ***: p=<0.001

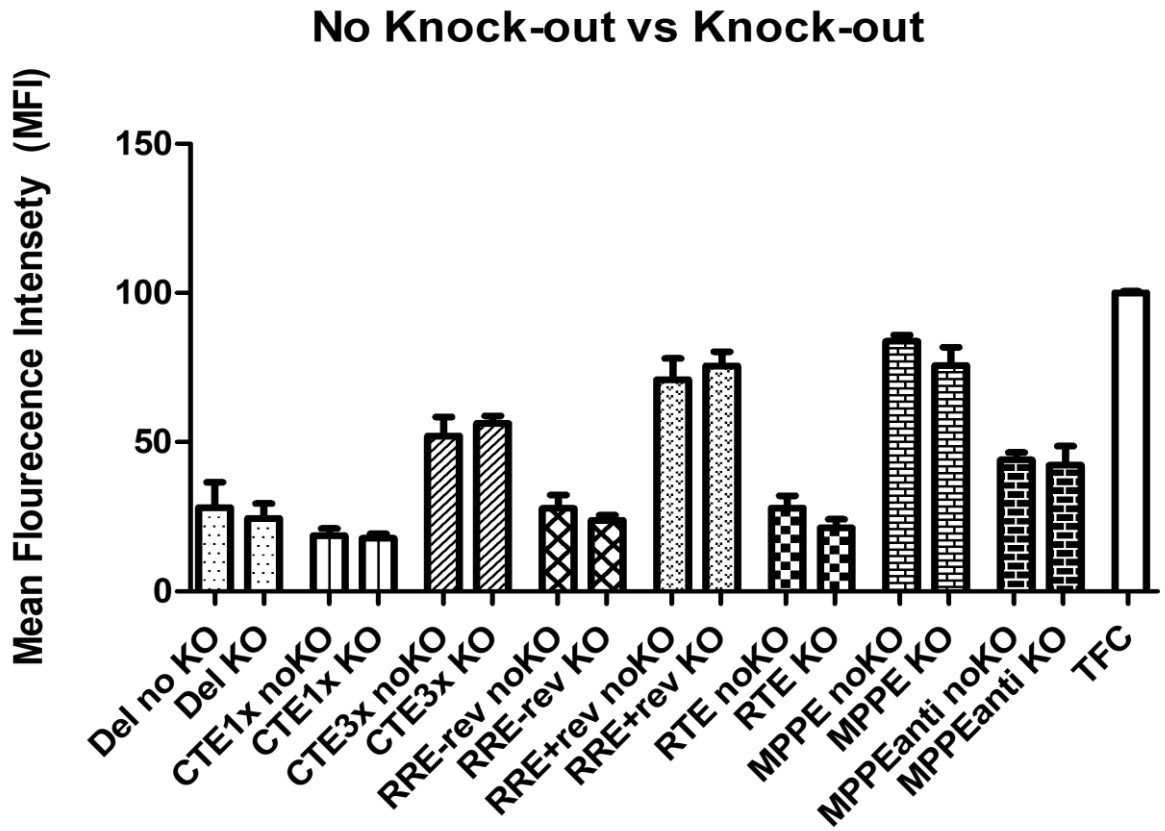

Figure 12: comparison of MFI between no knock.out and knock-out of different p3C-CmVt10CuOeGFPpA: MFI was normalized to transfection control (TFC) which was transfected with a constitutively expressing eGFP plasmid (pCMV-eGFP). No significant difference between no knock-out and knock-out group can be detected. Significance differences between the no knock-out group and knock-out group, within each reporter system, was calculated with a two-tailed, unpaired t-test for equal or unequal variances, depending on the outcome of previously performed F-test for equality of variances. *: p=<0.05, **: p=<0.01. ***: p=<0.001

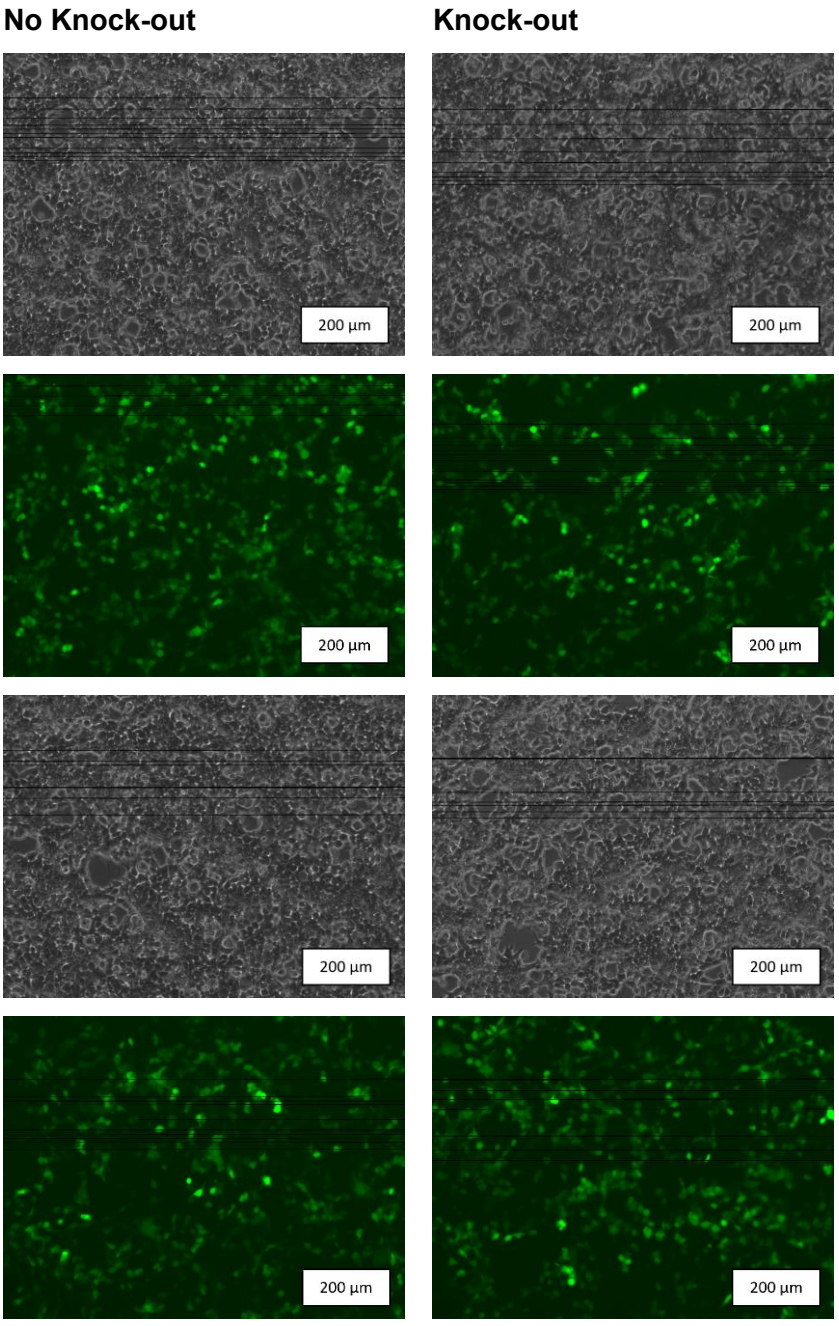
No Knock-out
Knock-out
200 µm
200 µm
200 µm
200 µm
200 µm
200 µm
200 µm
200 µm
p3C-CMVt10CuO.eGFPpA-del
p3C-CMVt10CuO.eGFPpA-CTE1x

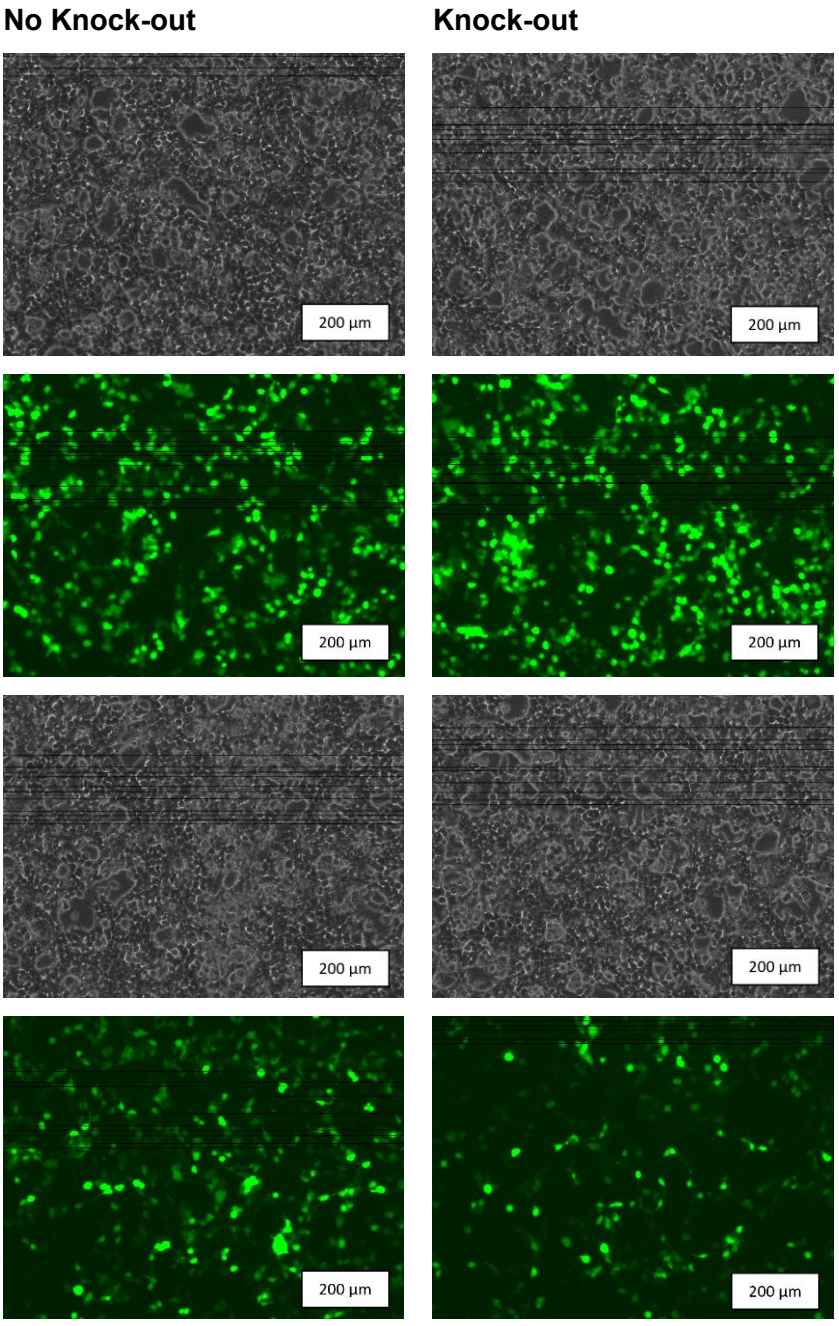
No Knock-out
Knock-out
200 µm
200 µm
200 µm
200 µm
200 µm
200 µm
200 µm
200 µm
p3C-CMVt10CuO.eGFPpA-CTE3x
p3C-CMVt10CuO.eGFPpA-RTE

No Knock-out **Knock-out**

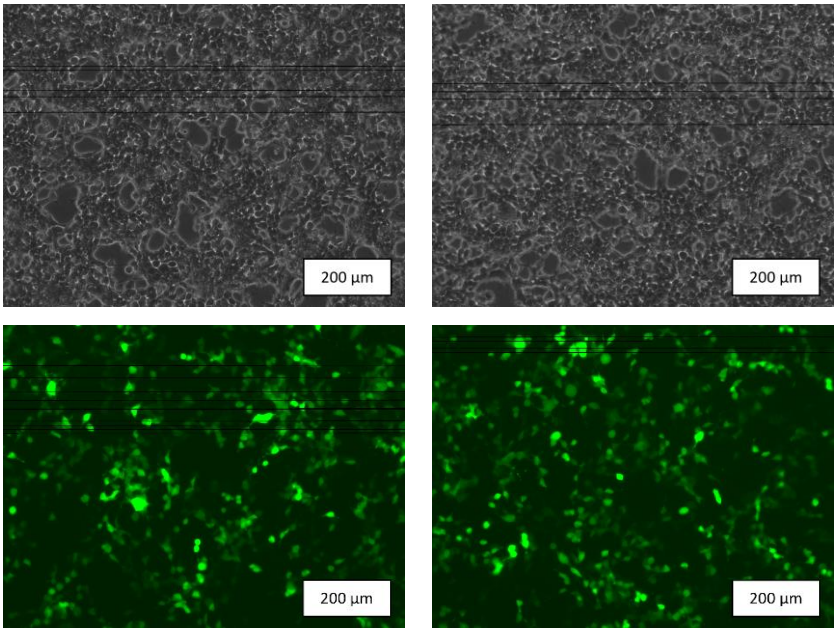

p3C-CMVt10CuO.eGFPpA-RRE without Rev

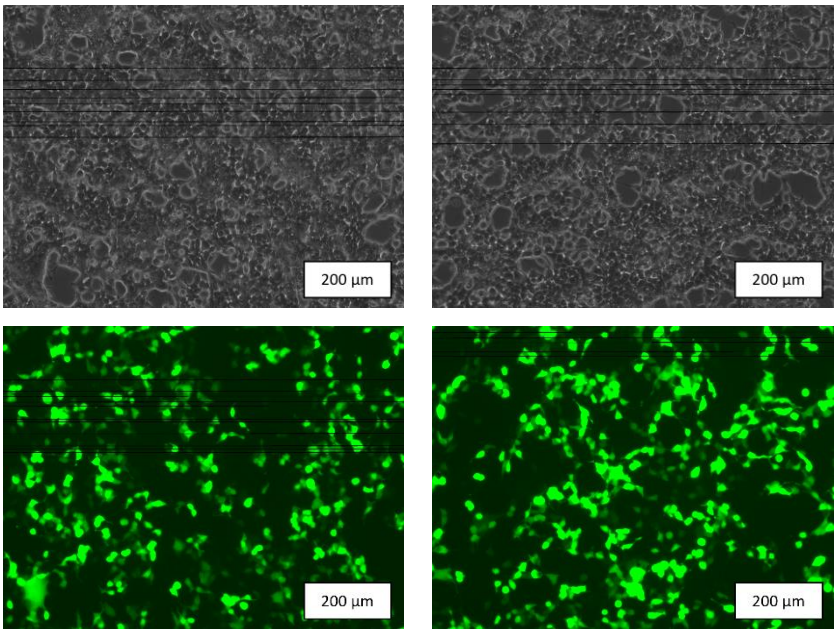

p3C-CMVt10CuO.eGFPpA-RRE with Rev

No Knock-out **Knock-out**

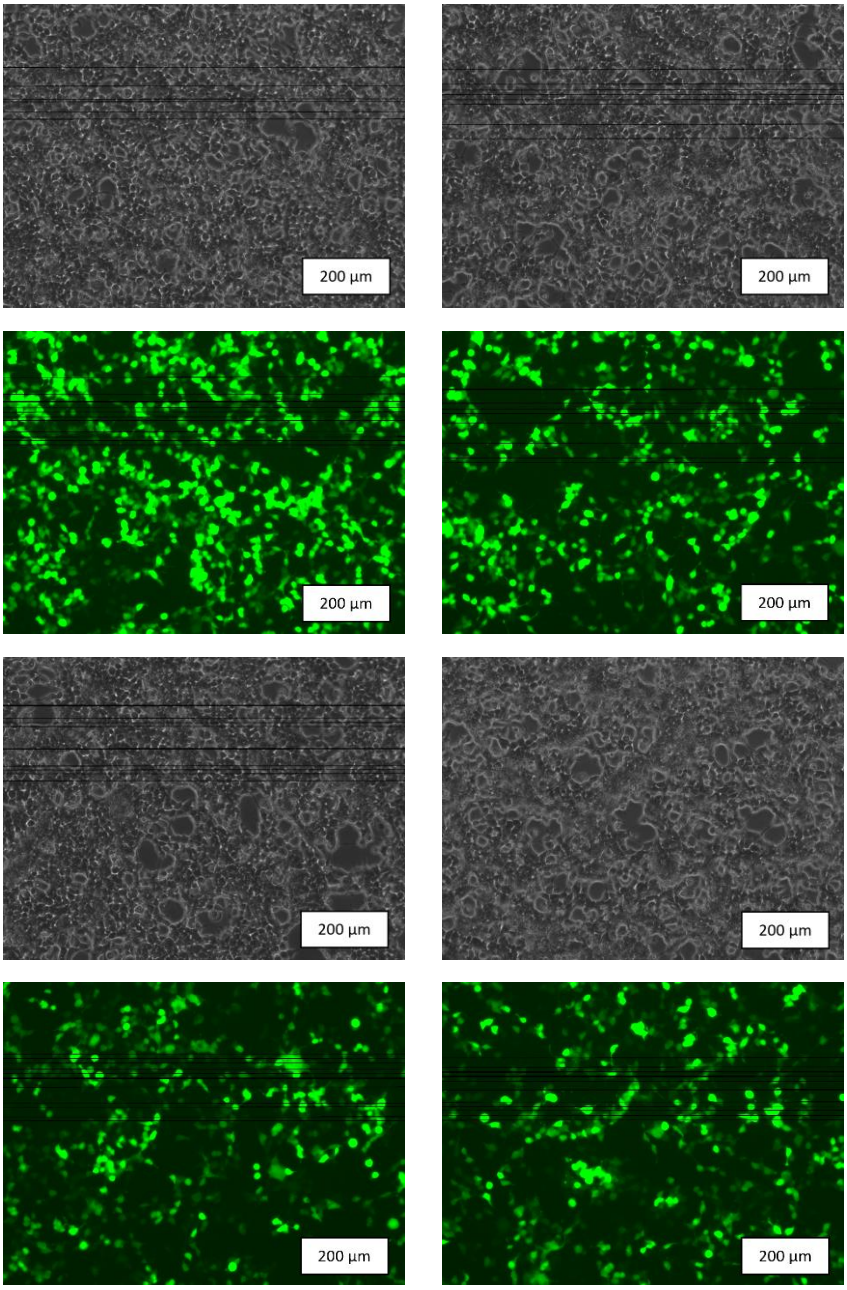

p3C-CMVt10CuO.eGFPpA-MPPE

p3C-CMVt10CuO.eGFPpA-MPPEanti

Figure 13 **eGFP expression levels of the different p3-CMVt10CuOΔ-eGFPpA reporter plasmids compared no *Mettl3* knock-out vs *Mettl3* kockout, assessed with fluorescence microscopy**: After transfecting the cells with the different reporter plasmids the expression was induced with cumate and doxycycline 24 hours post transfection. In the left column reporter plasmids were transduce into cells without a *Mettl3* knock-out, in the second column reporter plasmids were transduce into cells with *Mettl3* knock-out. Pictures were taken under brightfield illumination and under fluorescence excitation. As reflecting the results of the MFI measured in FACS, CTE3x, RRE with Rev and MPPE showing the brightest expression of eGFP

3.4 Influence of NXT1 and NXF1 overexpression on different export elements

3.4.1 3.2 Construction of the pBRY-NXT1-IRES-Puro plasmid

mRNA is transported from the nucleus to the cytoplasm. For this to happen the mRNA has to be transported through the nuclear pore complex (NPC) (15) . Different export adapters bind to mRNA and facilitate the export from the nucleus to the cytoplasm through different pathways. Additionally, nuclear export receptor proteins such as NXT1/NXF1 complex interacts with the mRNA/adapter complex and boosts the export (60, 61). The aim of these experiments was to find out if the overexpression of NXF1 together with NXT1 can boost the export of transcripts carrying various export elements.

We obtained the human NXF1 expression plasmid from another working group. Our group, on the other hand, created expression construct for the human NXT1. The human NXT1 gene was cloned into the pBRY-NXT1-IRES-Puro plasmid. To double check, if the gene inside the plasmid was really the human NXT1 gene, it was blasted on the NCBI homepage. Figure 14 shows the result of the nucleotide blast (nBlast) and confirms that the cloning was successful.

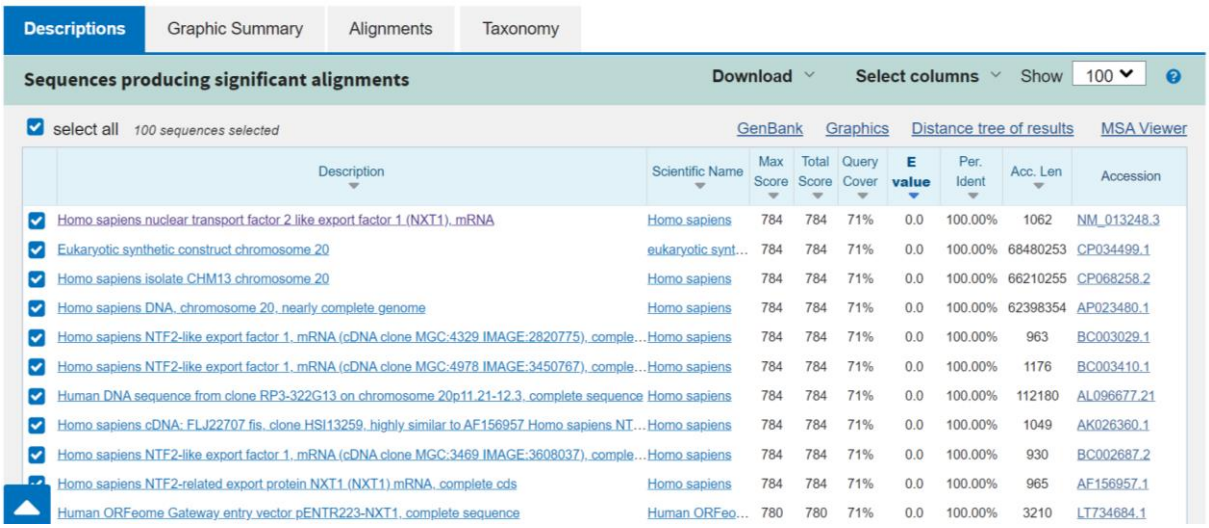

Description	Scientific Name	Max Score	Total Score	Query Cover	E value	Per. Ident	Acc. Len	Accession
Homo sapiens nuclear transport factor 2 like export factor 1 (NXT1), mRNA	Homo sapiens	784	784	71%	0.0	100.00%	1062	NM_013248.3
Eukaryotic synthetic construct chromosome 20	eukaryotic synt...	784	784	71%	0.0	100.00%	68480253	CP034499.1
Homo sapiens isolate CHM13 chromosome 20	Homo sapiens	784	784	71%	0.0	100.00%	66210255	CP068258.2
Homo sapiens DNA, chromosome 20, nearly complete genome	Homo sapiens	784	784	71%	0.0	100.00%	62398354	AP023480.1
Homo sapiens NTF2-like export factor 1, mRNA (cDNA clone MGC:4329 IMAGE:2820775), comple...	Homo sapiens	784	784	71%	0.0	100.00%	963	BC003029.1
Homo sapiens NTF2-like export factor 1, mRNA (cDNA clone MGC:4978 IMAGE:3450767), comple...	Homo sapiens	784	784	71%	0.0	100.00%	1176	BC003410.1
Human DNA sequence from clone RP3-322G13 on chromosome 20p11.21-12.3, complete sequence	Homo sapiens	784	784	71%	0.0	100.00%	112180	AL096677.21
Homo sapiens cDNA: FLJ22707 fis, clone HSI13259, highly similar to AF156957 Homo sapiens NT...	Homo sapiens	784	784	71%	0.0	100.00%	1049	AK026360.1
Homo sapiens NTF2-like export factor 1, mRNA (cDNA clone MGC:3469 IMAGE:3608037), comple...	Homo sapiens	784	784	71%	0.0	100.00%	930	BC002687.2
Homo sapiens NTF2-related export protein NXT1 (NXT1) mRNA, complete cds	Homo sapiens	784	784	71%	0.0	100.00%	965	AF156957.1
Human ORFeome Gateway entry vector pENTR223-NXT1, complete sequence	Human ORFeo...	780	780	71%	0.0	100.00%	3210	LT734684.1

Figure 14: Result of the nBlast of NXT1: Result of the nucleotide blast (nBlast) with the sequenced human NXT1 within the plasmid used for this work. The “Query cover” describes how much of the query matches the blast sequence, in percentage. In this case, 71 % of the query sequence align with the blast sequences. As we haven’t sent the complete human NXT1 coding region for sequencing it’s impossible to reach 100% of the ‘Query cove’. The ‘Percentage identity’ on the other hand gives the

percentage of how much of the nucleotide sequence aligns with the blast sequence. 100% of our provided sequence aligns with the human NXT1 gene provided by other research groups. The ‘E-Value’ describes the chance of how likely it is for our sequence to match randomly. As the E value for the best hints is 0, it is not likely for a false positive alignment with the human NXT1. In conclusion, it is proven with this nBlast, that our coding hNXT1 is indeed human and should produce the right protein.

Figure 15: Graphical overview of the nBlast of NXT1**:** a) shows a graphic overview of the nBlast, the horizontal bars are colour coded with the colour red giving the highest alignment score. b) The close-up alignment comparing the provided sequence to the top hit of this nBlast. All bases pair up between provided and top result. Which confirms that the *NXT1* gen inside the pBRY-NXT1-IRES-Puro plasmid is indeed the human *NXT1* gen

3.4.2 Effect of NXT1 and/or NXF1 overexpression on the eGFP expression from plasmids carrying various RNA export elements

Various groups have shown that overexpression of NXT1 and NXF1 or a combination of both enhance the export from the nucleus to the cytoplasm of mRNA containing export elements such as CTE or RTE (62, 63). Thus, we wanted to see if we can recapitulate the results of others with our reporter system. Furthermore, we wanted to find out if we can enhance expression of the MPPE-containing reporter mRNA.

First step was to calibrate the setup to find the right amount of NXT1/NXF1 (Data not shown). After determining what the best concentration of NXT1/NXF1 is, we decided to continue with 40ng of NXT1 and 100ng of NXF1. Combining the reporter construct, as described above, with NXT1 and/or NXF1.

All the data was normalized to p3C-CMVt10CuOeGFPpA-del without any NXT1 or NXF1. The significance of difference between export element with additional NXT1, NXF1 or a combination of both was calculated with an unpaired t-test for equal or unequal variance, depending on the outcome of previously performed F-test for equality of variances.

As shown in Figure 16 no statistically significant difference between all variations can be observed looking at the percentage of eGFP positive cells. p3C-CMVt10CuOeGFPpA-CTE3x and p3C-CMVt10CuOeGFPpA-MPPE give a slightly higher amount of eGFP positive cells compared to the other export elements.

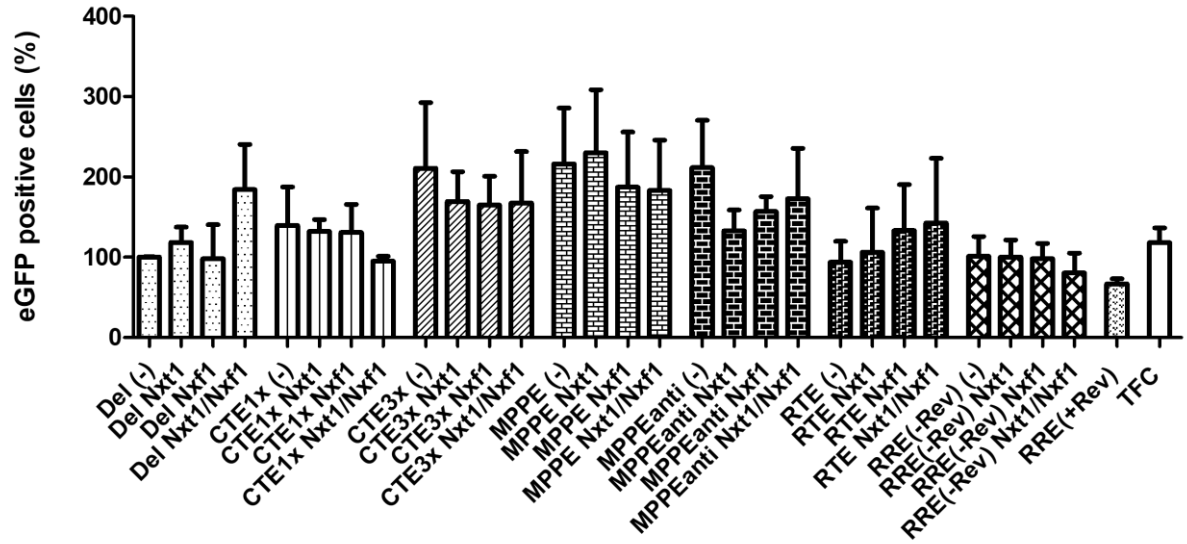

Figure 16: eGFP positive cell count of different p3C-CMVt10CuOeGFPpA reporter elements. Comparing the influence of NXT1 or/and NXF1 to the control group: eGFP positive cells were normalized to the reporter plasmid without any export element and no additional NXT1 or NXF1. No significant difference between each group can be detected. Significance differences between (-) and NXT1 or/and NXF1, within each reporter system, was calculated with a two-tailed, unpaired t-test for equal or unequal variances, depending on the outcome of previously performed F-test for equality of variances. *: p=<0.05, **: p=<0.01. ***: p=<0.001

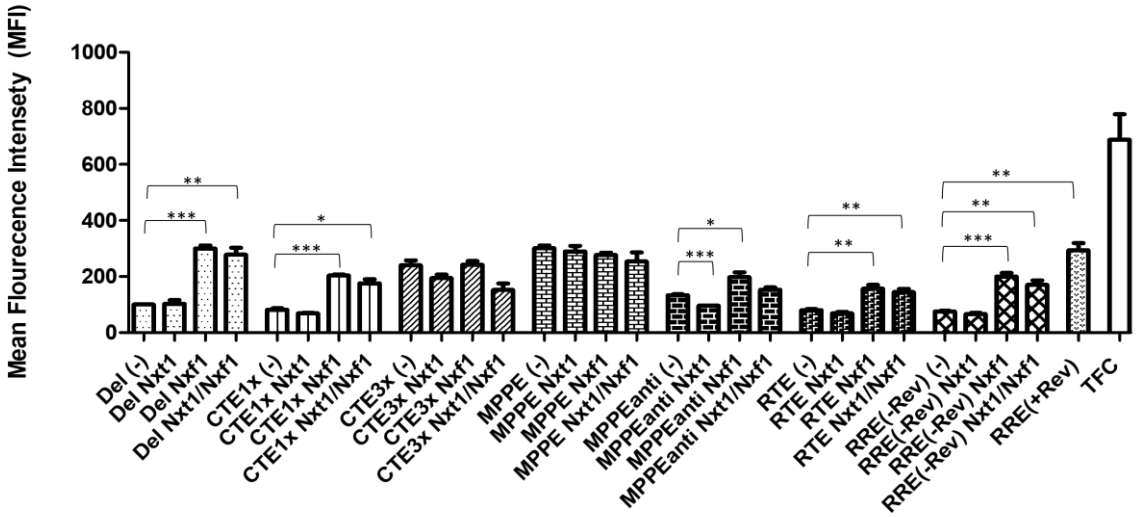

Figure 17: comparing eGFP expression level through the MFI: MFI was normalized to the reporter plasmid without any export element and no additional NXT1 or NXF1. Significant enhancement of eGFP expression could be measured with NXF1 in the empty reporter system p3C-CmVt10CuOeGFPpA-del, p3C-CmVt10CuOeGFPpA-CTE1x, p3C-CmVt10CuOeGFPpA-MPPEanti, p3C-CmVt10CuOeGFPpA-RTE and p3C-CmVt10CuOeGFPpA-RRE without Rev. p3C-CmVt10CuOeGFPpA-RRE with Rev shows significantly enhanced eGFP expression compared to the p3C-CmVt10CuOeGFPpA-RRE without Rev. Combination of NXT1 and NXF1 enhances eGFP expression in following reporter systems: Del, CTE1x, RTE and RRE without Rev. Additionally, a significant difference between NXT1 and (-) could be observed in MPPEanti with (-) having the stronger expression than NXT1. Significance differences between (-) and NXT1 or/and NXF1, within each reporter system, was calculated with a two-tailed, unpaired t-test for equal or unequal variances, depending on the outcome of previously performed F-test for equality of variances. *: p=<0.05, **: p=<0.01. ***: p=<0.001.

Having a look at the MFI: the overexpression of NXT1 alone doesn't cause a significant increase in eGFP expression. With p3C-CMVt10CuOeGFPpA-MPPEanti a significant difference between control and NXT1 group can be observed, but the control is having the stronger eGFP expression compared to the NXT1 group. In contrast, overexpression of NXF1 gives a boost in eGFP expression for the following export elements: p3C-CMVt10CuOeGFPpA-(-), p3C-CMVt10CuOeGFPpA-CTE1x, p3C-CMVt10CuOeGFPpA-RTE, p3C-CMVt10CuOeGFPpA-RRE (without Rev) and p3C-CMVt10CuOeGFPpA-MPPEanti. With this export elements a significant difference between control group and group with additional NXF1 was measured.

The overexpression of both factors, NXT1/NXF1, shows a significant increase of eGFP expression in the same export elements as mentioned above for the NXF1 overexpression. The only exception was p3C-CMVt10CuOeGFPpA-MPPEanti construct. However, simultaneous overexpression of NXT1/NXF1 had a smaller impact on eGFP expression than overexpression of the NXF1 alone.

Consistent with previous work of many groups, we observed a significant difference in eGFP expression of cells transfected with p3C-CMVt10CuOeGFPpA-RRE alone and with p3C-CMVt10CuOeGFPpA-RRE together with Rev.

4 Discussion

Our hypothesis was that the *Mettl3* knockout will have a negative effect on the viral RNA export from the nucleus into the cytoplasm. As a result of the crippled RNA export, the infectivity of Mouse Mammary Tumor Virus would be reduced. The decrease in virus production would be detected on agarose gel as a less intense PCR product from extracts obtained from the infected Mettl3 knockout cells. Importantly, we have not observed a marked difference in the intensities of the PCR products, see Figure 10.

CRISPR/Cas9 is a precise and efficient tool to manipulate DNA sequences. This system uses a guide RNA to direct the Cas9 endonuclease enzyme to the specific location on the DNA. It creates double stranded breaks that is repaired by the cellular repair mechanisms. These repairs include several nucleotides randomly inserted or deleted in the targeted region, causing a frame shift and ultimately a gene knockout (55). For targeting of the specific region in the genome, the design of sgRNA it is very important. To achieve a high knockout rate, several recommendations have to be followed (64–66). Some of our highly efficient sgRNAs follow those suggestions to some extent other following the suggestions show a low knockout rate (see knockout rate table 1). With this observation, it can be assumed that optimal sgRNA design can vary depending on organism and target sequence. Therefore, careful consideration of the nucleotide composition of the sgRNA sequence is necessary to ensure optimal performance and minimize off-target effects.

The determined knockout rate estimated by Synthego (https://ice.synthego.com/)) consist of the sum of all individual indels calculated by their program. Important to note is that the indels must be checked to cause a frame shift. If they don't cause a frame shift, but only delete one or more amino acid (deletion of -3 bases etc.), the function of the resulting protein will not be fully disrupted and can't therefore be included into the final knockout rate Figure 4-Figure 9.

The first assessment of the knockout rate of our guide RNAs showed a higher knockout rate (around 80%, see Table 2) compared to the final experiments where the cells were transfected also with the export element reporter system (see Figure 7). First, assessing the knockout rate of the various sgRNA was determined one days after transduction with the CRISPR/Cas 9 system causing the knockout. In contrast, the knockout rate for the final experiments was determined four days after transduction with CRISPR Cas9 due to the needed transfection with the export element reporter system. We speculated that these four additional days gave

the cells without a knockout time to grow faster than cells with *Mettl3* knockout and therefore to lower the final knockout rate. *Mettl3* is an essential gene and cells with knockout therefore show a growth disadvantage to wild type cells (4)

The ratio of eGFP positive cells between all reporter system is within a range of 18% and 25%. Showing the efficiency of the transfection with the different reporter constructs is about the same for every system. Having no significant difference in eGFP positive cells between no knockout group and knockout group imply that there is no effect of the knockout to our transfection efficiency. Visually a tendency for a lower proportion of eGFP expressing cells can be observed within most knockout groups but it isn't statistically significantly lower.

eGFP expression levels, on the other hand, gets influenced by the different reporter plasmids caring the different export elements. Three copies of CTE in p3C-CMVt10CuOeGFPpA-CTE3x and MPPE in p3C-CMVt10CuOeGFPpA-MPPE show the highest eGFP expression levels. A strong eGFP signal can be also obtained when RRE is present in the reporter construct and Rev is co-expressed. This result reflects previous studies were Rev was identified to form a complex with RRE to facilitate the transit of viral RNA into the cytoplasm. (67, 68). In the absence of Rev no increase of eGFP expression compared to the control can be observed. MPPE in anti-sense direction shows moderate eGFP expression compared to the control, without any export element p3C-CMVt10CuOeGFPpA-(del). These findings are consistent with the results obtained during the development of this constructs by MSc student Bernhard Willdom in the Indik's group.

After evaluating that the reporter system is functioning, the influence of the *Mettl3* knockout was evaluated. In contrast to previous work (14) no significant difference between knockout and no knockout group in terms mRNA export could be observed in neither of the reporter system constructs.

Methylation is carried out inside the nucleus by an enzyme heterodimer formed by methyl transferase 3 (METTL3) and methyl transferase 14 (METTL14) (6) Even though there are several enzymes involved in the methylation process recent studies shows that with a knockout of the *Mettl3* gene a reduction of 90% of m6A levels can occur (69). Not only for cellular mRNA, methylation plays an important role in delivering information and export from the nucleus into the cytoplasm but for viral mRNA too. The m6A modification of viral mRNA has been reported for several viruses whose replication cycle involves the nucleus, including retroviruses (70). Therefore, we hypothesised that there should be a difference in the viral mRNA export and

therefore in turn, in the eGFP expression levels from our reporter constructs carrying the viral elements. In comparison to our findings.

We speculate that the lack of detectable difference in the nuclear export activity could be due to a low knockout rate (around 60%) observed in our transfection experiments. We generated an inducible system were the *Mettl3* gene could be transfected via plasmid and induced externally which would result in *Mettl3* expression during transfection with the reporter system. The cell line going to be used have no functioning *Mettl3* gene, so the knockout rate would be 100 %. Unfortunately, this would have gone beyond the scope of the project and therefore could be a future project.

The mRNA transport is not only influenced by the RNA methylation but also by the cellular proteins involved in this process. The transcription-export complex 1 (TREX1) recruits NXFT1/NXF1 (71) and build a pathway manly used to transport mRNA into the cytoplasm (72). The exportin 1, also known as chromosome region maintenance 1 (CRM1) (73), mainly exports cellular proteins, ribosomal RNA subunits and non-coding RNAs. However, recent studies showed that CRM1 pathway is also used for mRNA export too (20).

Viruses hijack cellular machinery to replicate. They have developed mechanisms to be able to transport viral RNA or proteins into the nucleus and to export viral proteins and RNA back into the cytoplasm. Various viruses use RNA structural elements, which interacts with the cellular export proteins to transport their RNA molecules into the cytoplasm (74). The viral export elements used in this work are RRE, CTE, RTE and MPPE. The CTE and RTE are interacting with NXT1/NXF1 to facilitate the export of viral product out of the nucleus (26, 75, 12). In contrast RRE interacts with CRM1 through the help of Rev to facilitate the export of viral RNA through the NPC (76).

We hypothesised that by overexpressing the NXT1/NXF1 proteins, the eGFP expression levels from constructs carrying export elements exported with the help of the export receptor heterodimer will be enhanced. We were especially interested in a novel export element MPPE (data unpublished) whose export pathway has not been characterized.

Our results are showed that CTE1x, RTE and RRE without Rev are having all nearly the same eGFP expression as our control without any export element. They even show a slight decrease in MFI compared to the control. None of those RNA export elements can increase the eGFP

expression levels above the background level. It was shown in previous studies that one copy of CTE is not able to enhance eGFP expression above background levels. In these studies, at least three copies of CTE were needed to elevate eGFP expression to detectible levels. (4, 77). Which our findings reflect.

The construct carrying CTE3x is showing a high eGFP expression even without NXT1/NXF1 and no considerable influence of NXF1 can be observed. Which leads to the conclusion that three copies of CTE already elevates mRNA export to its limit and NXF1 will not have a significant effect.

RTE and CTE are very similar in their structure, therefore RTE also uses the NXF1 pathway for RNA export. In this case an adaptor RMB15 is used to bridge interaction with NXF1/NXT1 (12). RTE isn't showing a significant increase in eGFP expression compared to control. This could be due to being structural and functional similar to CTE, hence introduction multiple copies of RTE into the construct could bring an elevated eGFP expression.

No effect on RRE without Rev is not surprising, as RRE needs Rev to facilitate the interaction to CRM1 pathway (78). Without providing any Rev to interact with, the eGPF expression is staying at background level. A significant difference between RRE without and with Rev can be seen (p-value: 0,0011).

All three export-element constructs behave the same as the control when co-transfected with NXT1, NXF1 or NXT1/NXF1. The NXF1 and NXT1/NXF1 overexpression results in a significant increase in eGFP expression. As previously established a boost with NXF1 is increasing mRNA export through the NXF1 pathway (63). Due the fact that we weren't able to distinguish between background level and influence of CTE1x and RTE we can't reproduce previous finding were NXF1 is boosting mRNA export and with that eGFP expression, through the CMR1 pathway.

Unexpectedly, we observed that overexpression of NXT1 slightly suppressed mRNA export. This phenomenon was observed for all constructs carrying various export elements even in combination with NXF1. No paper can be found saying why this could be.

The aim of the NXT1/NXF1 expression experiments was to find out whether the novel RNA export elements from MMTV, MPPE, (data not published) will be influenced by the NXT1 and NXF1. The results should give us a hint on which pathway MPPE is using for mRNA export. Unfortunately, eGFP expression is even without NXT1/NXF1 as high as with constructs

carrying CTE3x and RRE+Rev. As no influence of NXF1 can be observed with construct containing CTE3x we assume that even if MPPE interacts with NXF1, no positive effect will be visible because of reaching the upper limit of the mRNA export assay.

MPPE in antisense on the other hand shows a boost in eGFP expression with NXF1 but it's the same with the control. Because of MPPE in antisense is not going to create a functioning protein this positive influence of NXF1 is likely background noise.

In summary we couldn't find any significant impact of *Mettl3* knockout to viral mRNA export. But adjusting the setup of the project could lead to a positive result.

Having NXT1/NXF1 boosting mRNA export elements which use the CRM1 pathway could not fully reproduced, like done in several other publications. Modifying our system is strongly suggested.

Literature Cited

1. Dunin-Horkawicz S, Czerwoniec A, Gajda MJ, Feder M, Grosjean H, Bujnicki JM. MODOMICS: a database of RNA modification pathways. Nucleic Acids Res 2006; 34(Database issue):D145-9.

2. Li S, Mason CE. The pivotal regulatory landscape of RNA modifications. Annu Rev Genomics Hum Genet 2014; 15:127–50.

3. Roignant J-Y, Soller M. m6A in mRNA: An Ancient Mechanism for Fine-Tuning Gene Expression. Trends in Genetics 2017; 33(6):380–90.

4. Wodrich H, Schambach A, Kräusslich HG. Multiple copies of the Mason-Pfizer monkey virus constitutive RNA transport element lead to enhanced HIV-1 Gag expression in a context-dependent manner. Nucleic Acids Res 2000; 28(4):901–10.

5. Batista PJ, Molinie B, Wang J, Qu K, Zhang J, Li L et al. m(6)A RNA modification controls cell fate transition in mammalian embryonic stem cells. Cell Stem Cell 2014; 15(6):707–19.

6. Liu J, Yue Y, Han D, Wang X, Fu Y, Zhang L et al. A METTL3-METTL14 complex mediates mammalian nuclear RNA N6-adenosine methylation. Nat Chem Biol 2014; 10(2):93–5.

7. Schwartz S, Mumbach MR, Jovanovic M, Wang T, Maciag K, Bushkin GG et al. Perturbation of m6A writers reveals two distinct classes of mRNA methylation at internal and 5' sites. Cell Rep 2014; 8(1):284–96.

8. Dominissini D, Moshitch-Moshkovitz S, Schwartz S, Salmon-Divon M, Ungar L, Osenberg S et al. Topology of the human and mouse m6A RNA methylomes revealed by m6A-seq. nature 2012; 485(7397):201–6.

9. Zhou Y, Kong Y, Fan W, Tao T, Xiao Q, Li N et al. Principles of RNA methylation and their implications for biology and medicine. Biomed Pharmacother 2020; 131:110731.

10. Xiao W, Adhikari S, Dahal U, Chen Y-S, Hao Y-J, Sun B-F et al. Nuclear m(6)A Reader YTHDC1 Regulates mRNA Splicing. Mol Cell 2016; 61(4):507–19.

11. Roundtree IA, Luo G-Z, Zhang Z, Wang X, Zhou T, Cui Y et al. YTHDC1 mediates nuclear export of N6-methyladenosine methylated mRNAs. Elife 2017; 6.

12. Lindtner S, Zolotukhin AS, Uranishi H, Bear J, Kulkarni V, Smulevitch S et al. RNA-binding motif protein 15 binds to the RNA transport element RTE and provides a direct link to the NXF1 export pathway. J Biol Chem 2006; 281(48):36915–28.

13. Jia G, Fu Y, Zhao X, Dai Q, Zheng G, Yang Y et al. N6-methyladenosine in nuclear RNA is a major substrate of the obesity-associated FTO. Nat Chem Biol 2011; 7(12):885–7.

14. Lichinchi G, Gao S, Saletore Y, Gonzalez GM, Bansal V, Wang Y et al. Dynamics of the human and viral m 6 A RNA methylomes during HIV-1 infection of T cells. Nat Microbiol 2016; 1(4):1–9. Available from: URL: https://www.nature.com/articles/nmicrobiol201611.pdf.

15. Alberts B. Molecular biology of the cell. 6.ed. New York, Abingdon: Garland Science, Taylor and Francis; 2015.

16. Delaleau M, Borden KLB. Multiple Export Mechanisms for mRNAs. Cells 2015; 4(3):452–73.

17. Lim RYH, Fahrenkrog B, Köser J, Schwarz-Herion K, Deng J, Aebi U. Nanomechanical basis of selective gating by the nuclear pore complex. Science 2007; 318(5850):640–3.

18. Bischoff FR, Görlich D. RanBP1 is crucial for the release of RanGTP from importin beta-related nuclear transport factors. FEBS Lett 1997; 419(2-3):249–54.

19. Gales JP, Kubina J, Geldreich A, Dimitrova M. Strength in Diversity: Nuclear Export of Viral RNAs. Viruses 2020; 12(9).

20. Hutten S, Kehlenbach RH. CRM1-mediated nuclear export: to the pore and beyond. Trends in cell biology 2007; 17(4):193–201. Available from: URL: https://pubmed.ncbi.nlm.nih.gov/17317185/.

21. Rougemaille M, Dieppois G, Kisseleva-Romanova E, Gudipati RK, Lemoine S, Blugeon C et al. THO/Sub2p functions to coordinate 3'-end processing with gene-nuclear pore association. Cell 2008; 135(2):308–21.

22. Cheng H, Dufu K, Lee C-S, Hsu JL, Dias A, Reed R. Human mRNA export machinery recruited to the 5' end of mRNA. Cell 2006; 127(7):1389–400.

23. Hautbergue GM, Hung M-L, Golovanov AP, Lian L-Y, Wilson SA. Mutually exclusive interactions drive handover of mRNA from export adaptors to TAP. Proc Natl Acad Sci U S A 2008; 105(13):5154–9.

24. Jani D, Valkov E, Stewart M. Structural basis for binding the TREX2 complex to nuclear pores, GAL1 localisation and mRNA export. Nucleic Acids Res 2014; 42(10):6686–97.

25. Valkov E, Dean JC, Jani D, Kuhlmann SI, Stewart M. Structural basis for the assembly and disassembly of mRNA nuclear export complexes. Biochim Biophys Acta 2012; 1819(6):578–92.

26. Braun IC, Herold A, Rode M, Conti E, Izaurralde E. Overexpression of TAP/p15 heterodimers bypasses nuclear retention and stimulates nuclear mRNA export. J Biol Chem 2001; 276(23):20536–43.

27. Katahira J, Straesser K, Saiwaki T, Yoneda Y, Hurt E. Complex formation between Tap and p15 affects binding to FG-repeat nucleoporins and nucleocytoplasmic shuttling. J Biol Chem 2002; 277(11):9242–6.

28. Coffin JM, Hughes SH, Varmus HE, editors. Retroviruses. Cold Spring Harbor Laboratory Press; 1997.

29. Liechtenstein T, Perez-Janices N, Escors D. Lentiviral vectors for cancer immunotherapy and clinical applications. Cancers (Basel) 2013; 5(3):815–37.

30. Charnay N, Ivanyi-Nagy R, Soto-Rifo R, Ohlmann T, López-Lastra M, Darlix J-L. Mechanism of HIV-1 Tat RNA translation and its activation by the Tat protein. Retrovirology 2009; 6:74.

31. Harwig A, Jongejan A, van Kampen AHC, Berkhout B, Das AT. Tat-dependent production of an HIV-1 TAR-encoded miRNA-like small RNA. Nucleic Acids Res 2016; 44(9):4340–53.

32. Cullen BR. Retroviruses as model systems for the study of nuclear RNA export pathways. Virology 1998; 249(2):203–10.

33. Bray M, Prasad S, Dubay JW, Hunter E, Jeang KT, Rekosh D et al. A small element from the Mason-Pfizer monkey virus genome makes human immunodeficiency virus type 1 expression and replication Rev-independent. Proc Natl Acad Sci U S A 1994; 91(4):1256–60.

34. Pasquinelli AE, Ernst RK, Lund E, Grimm C, Zapp ML, Rekosh D et al. The constitutive transport element (CTE) of Mason-Pfizer monkey virus (MPMV) accesses a cellular mRNA export pathway. EMBO J 1997; 16(24):7500–10.

35. Kang Y, Cullen BR. The Human Tap Protein Is a Nuclear mRNA Export Factor That Contains Novel RNA-binding and Nucleocytoplasmic Transport Sequences. Genes Dev 1999; 13(9).

36. Aibara S, Katahira J, Valkov E, Stewart M. The principal mRNA nuclear export factor NXF1:NXT1 forms a symmetric binding platform that facilitates export of retroviral CTE-RNA. Nucleic Acids Res 2015; 43(3):1883–93.

37. Reddy TR, Tang H, Xu W, Wong-Staal F. Sam68, RNA helicase A and Tap cooperate in the post-transcriptional regulation of human immunodeficiency virus and type D retroviral mRNA. Oncogene 2000; 19(32):3570–5.

38. Zolotukhin AS, Michalowski D, Smulevitch S, Felber BK. Retroviral constitutive transport element evolved from cellular TAP(NXF1)-binding sequences. J Virol 2001; 75(12):5567–75.

39. Nappi F, Schneider R, Zolotukhin A, Smulevitch S, Michalowski D, Bear J et al. Identification of a novel posttranscriptional regulatory element by using a rev- and RRE-mutated human immunodeficiency virus type 1 DNA proviral clone as a molecular trap. J Virol 2001; 75(10):4558–69.

40. Sakuma T, Tonne JM, Ikeda Y. Murine leukemia virus uses TREX components for efficient nuclear export of unspliced viral transcripts. Viruses 2014; 6(3):1135–48.

41. Malim MH, Hauber J, Fenrick R, Cullen BR. Immunodeficiency virus rev trans-activator modulates the expression of the viral regulatory genes. nature 1988; 335(6186):181–3.

42. Fornerod M, Ohno M, Yoshida M, Mattaj IW. CRM1 is an export receptor for leucine-rich nuclear export signals. Cell 1997; 90(6):1051–60.

43. Bai Y, Tambe A, Zhou K, Doudna JA. RNA-guided assembly of Rev-RRE nuclear export complexes. Elife 2014; 3:e03656.

44. Yedavalli VSRK, Neuveut C, Chi Y-H, Kleiman L, Jeang K-T. Requirement of DDX3 DEAD box RNA helicase for HIV-1 Rev-RRE export function. Cell 2004; 119(3):381–92.

45. Tange TØ, Nott A, Moore MJ. The ever-increasing complexities of the exon junction complex. Curr Opin Cell Biol 2004; 16(3):279–84.

46. Blissenbach M, Grewe B, Hoffmann B, Brandt S, Uberla K. Nuclear RNA export and packaging functions of HIV-1 Rev revisited. J Virol 2010; 84(13):6598–604.

47. Malim MH, Böhnlein S, Fenrick R, Le SY, Maizel JV, Cullen BR. Functional comparison of the Rev trans-activators encoded by different primate immunodeficiency virus species. Proc Natl Acad Sci U S A 1989; 86(21):8222–6.

48. Phillips TR, Lamont C, Konings DA, Shacklett BL, Hamson CA, Luciw PA et al. Identification of the Rev transactivation and Rev-responsive elements of feline immunodeficiency virus. J Virol 1992; 66(9):5464–71.

49. Martarano L, Stephens R, Rice N, Derse D. Equine infectious anemia virus trans-regulatory protein Rev controls viral mRNA stability, accumulation, and alternative splicing. J Virol 1994; 68(5):3102–11.

50. Gomez Corredor A, Archambault D. The bovine immunodeficiency virus rev protein: identification of a novel lentiviral bipartite nuclear localization signal harboring an atypical spacer sequence. J Virol 2009; 83(24):12842–53.

51. Younis I, Green PL. The human T-cell leukemia virus Rex protein. Front Biosci 2005; 10:431–45.

52. Indik S, Günzburg WH, Salmons B, Rouault F. A novel, mouse mammary tumor virus encoded protein with Rev-like properties. Virology 2005; 337(1):1–6.

53. Mertz JA, Simper MS, Lozano MM, Payne SM, Dudley JP. Mouse mammary tumor virus encodes a self-regulatory RNA export protein and is a complex retrovirus. J Virol 2005; 79(23):14737–47.

54. Hohn O, Hanke K, Bannert N. HERV-K(HML-2), the Best Preserved Family of HERVs: Endogenization, Expression, and Implications in Health and Disease. Front Oncol 2013; 3:246.

55. Doudna JA, Charpentier E. Genome editing. The new frontier of genome engineering with CRISPR-Cas9. Science 2014; 346(6213):1258096.

56. Kim DH, Lee J, Suh Y, Lee K. Necessity for Validation of Effectiveness of Selected Guide RNA In Silico for Application of CRISPR/Cas9. Molecular biotechnology 2021; 63(2). Available from: URL: https://pubmed.ncbi.nlm.nih.gov/33386580/.

57. Indikova I, Indik S. Highly efficient 'hit-and-run' genome editing with unconcentrated lentivectors carrying Vpr.Prot.Cas9 protein produced from RRE-containing transcripts. Nucleic Acids Res 2020; 48(14):8178–87.

58. Bogerd HP, Echarri A, Ross TM, Cullen BR. Inhibition of human immunodeficiency virus Rev and human T-cell leukemia virus Rex function, but not Mason-Pfizer monkey virus constitutive transport element activity, by a mutant human nucleoporin targeted to Crm1. J Virol 1998; 72(11):8627–35.

59. Grüter P, Tabernero C, Kobbe C von, Schmitt C, Saavedra C, Bachi A et al. TAP, the human homolog of Mex67p, mediates CTE-dependent RNA export from the nucleus. Mol Cell 1998; 1(5):649–59.

60. Braun IC, Rohrbach E, Schmitt C, Izaurralde E. TAP binds to the constitutive transport element (CTE) through a novel RNA-binding motif that is sufficient to promote CTE-dependent RNA export from the nucleus. EMBO J 1999; 18(7):1953–65.

61. Kang Y, Cullen BR. The human Tap protein is a nuclear mRNA export factor that contains novel RNA-binding and nucleocytoplasmic transport sequences. Genes Dev 1999; 13(9):1126–39.

62. Jin L, Guzik BW, Bor Y-C, Rekosh D, Hammarskjöld M-L. Tap and NXT promote translation of unspliced mRNA. Genes Dev 2003; 17(24):3075–86.

63. Sasaki M, Takeda E, Takano K, Yomogida K, Katahira J, Yoneda Y. Molecular cloning and functional characterization of mouse Nxf family gene products. Genomics 2005; 85(5):641–53.

64. Doench JG, Hartenian E, Graham DB, Tothova Z, Hegde M, Smith I et al. Rational design of highly active sgRNAs for CRISPR-Cas9-mediated gene inactivation. Nat Biotechnol 2014; 32(12):1262–7.

65. Wu X, Scott DA, Kriz AJ, Chiu AC, Hsu PD, Dadon DB et al. Genome-wide binding of the CRISPR endonuclease Cas9 in mammalian cells. Nat Biotechnol 2014; 32(7):670–6.

66. Gagnon JA, Valen E, Thyme SB, Huang P, Akhmetova L, Pauli A et al. Efficient mutagenesis by Cas9 protein-mediated oligonucleotide insertion and large-scale assessment of single-guide RNAs. PLoS ONE 2014; 9(5):e98186.

67. Battiste JL, Mao H, Rao NS, Tan R, Muhandiram DR, Kay LE et al. Alpha helix-RNA major groove recognition in an HIV-1 rev peptide-RRE RNA complex. Science 1996; 273(5281):1547–51.

68. Malim MH, Tiley LS, McCarn DF, Rusche JR, Hauber J, Cullen BR. HIV-1 structural gene expression requires binding of the Rev trans-activator to its RNA target sequence. Cell 1990; 60(4):675–83.

69. Ke S, Pandya-Jones A, Saito Y, Fak JJ, Vågbø CB, Geula S et al. m6A mRNA modifications are deposited in nascent pre-mRNA and are not required for splicing but do specify cytoplasmic turnover. Genes Dev 2017; 31(10):990–1006.

70. Kane SE, Beemon K. Precise localization of m6A in Rous sarcoma virus RNA reveals clustering of methylation sites: implications for RNA processing. Mol Cell Biol 1985; 5(9):2298–306.

71. Viphakone N, Hautbergue GM, Walsh M, Chang C-T, Holland A, Folco EG et al. TREX exposes the RNA-binding domain of Nxf1 to enable mRNA export. Nat Commun 2012; 3:1006.

72. Viphakone N, Sudbery I, Griffith L, Heath CG, Sims D, Wilson SA. Co-transcriptional Loading of RNA Export Factors Shapes the Human Transcriptome. Mol Cell 2019; 75(2):310-323.e8.

73. Stade K, Ford CS, Guthrie C, Weis K. Exportin 1 (Crm1p) is an essential nuclear export factor. Cell 1997; 90(6):1041–50.

74. Koonin EV, Dolja VV, Krupovic M. Origins and evolution of viruses of eukaryotes: The ultimate modularity. Virology 2015; 479-480:2–25.

75. Guzik BW, Levesque L, Prasad S, Bor YC, Black BE, Paschal BM et al. NXT1 (p15) is a crucial cellular cofactor in TAP-dependent export of intron-containing RNA in mammalian cells. Mol Cell Biol 2001; 21(7):2545–54.

76. Vercruysse T, Daelemans D. HIV-1 Rev multimerization: mechanism and insights. Curr HIV Res 2013; 11(8):623–34.

77. Pocock GM, Becker JT, Swanson CM, Ahlquist P, Sherer NM. HIV-1 and M-PMV RNA Nuclear Export Elements Program Viral Genomes for Distinct Cytoplasmic Trafficking Behaviors. PLoS Pathog 2016; 12(4):e1005565.

78. Hammarskjöld ML. Regulation of retroviral RNA export. Semin Cell Dev Biol 1997; 8(1):83–90.